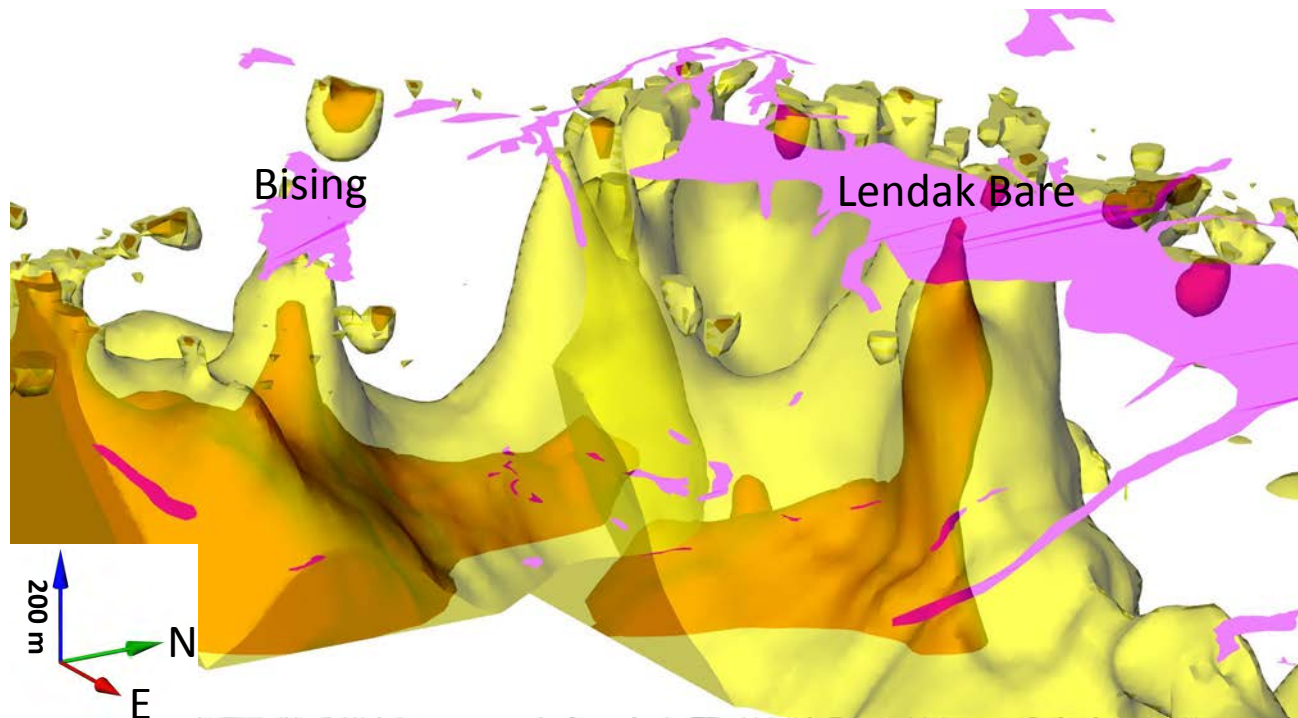


SW Lombok IUP:

Geological- and Geophysical-Interpretations,
Prospectivity Analysis and Porphyry Exploration Targets



Three-dimensional magnetic inversion models, silica-clay alteration zones and quartz-ledges (MSBs) in the Mencanggah area.

Presentation for Southern Arc Minerals

By Steve Garwin

13th December, 2011

Figure 1: Simplified geology for the SW Lombok IUP of Southern Arc Minerals, incorporating the results of the ongoing regional mapping program. The overlay shows a compilation of structural interpretations made by company geologists and the author.

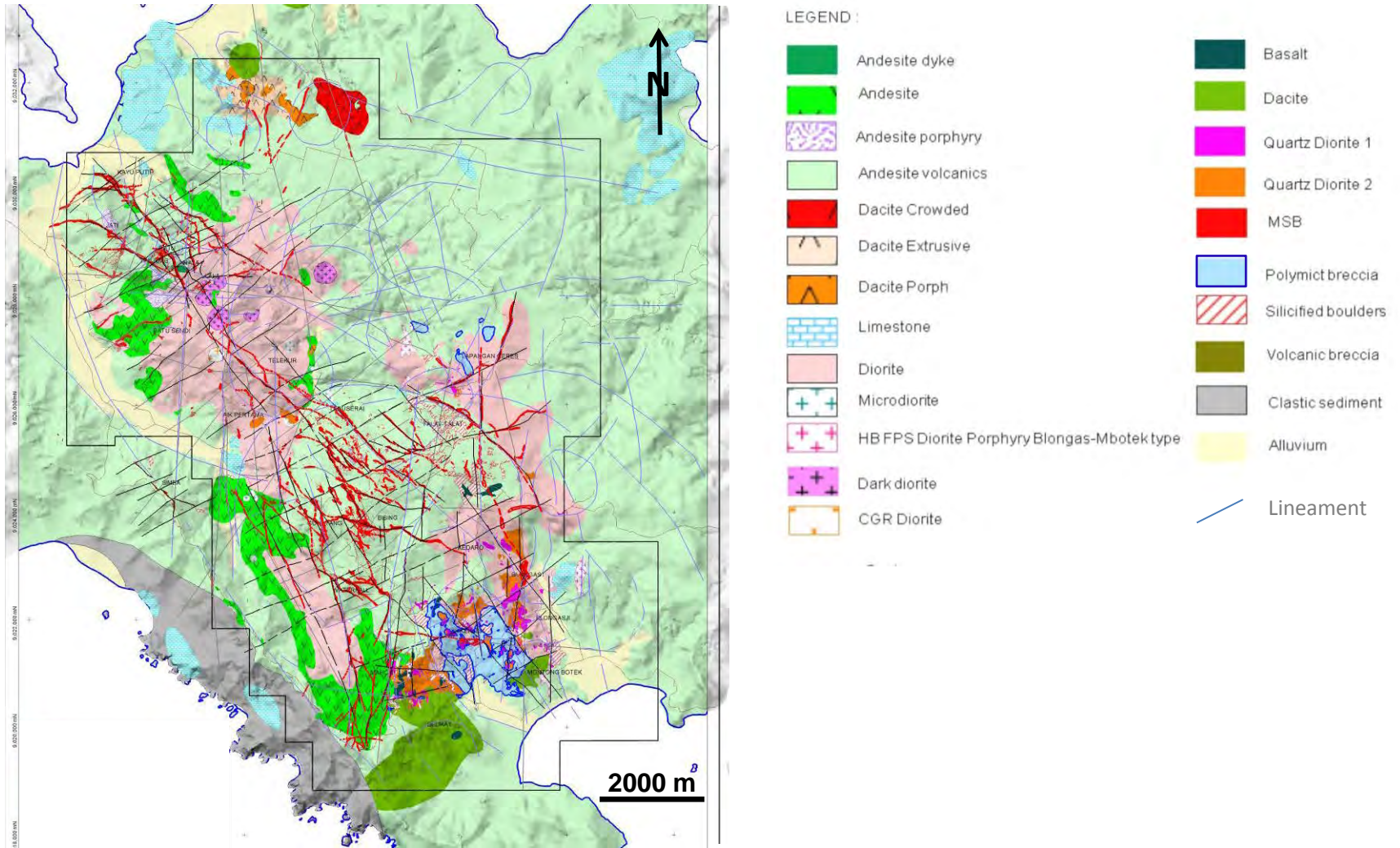


Figure 2: Simplified geology for the SW Lombok IUP of Southern Arc Minerals, incorporating the results of the ongoing regional mapping program and previous structural interpretations. The map shows a geological lineament interpretation based on the distribution of intrusions, quartz-ledges / MSBs and hydrothermal alteration zones. The lineaments (dark blue) are inferred to coincide with deep-seated faults and fracture zones that have guided the emplacement of intrusions and related hydrothermal alteration / mineralization.

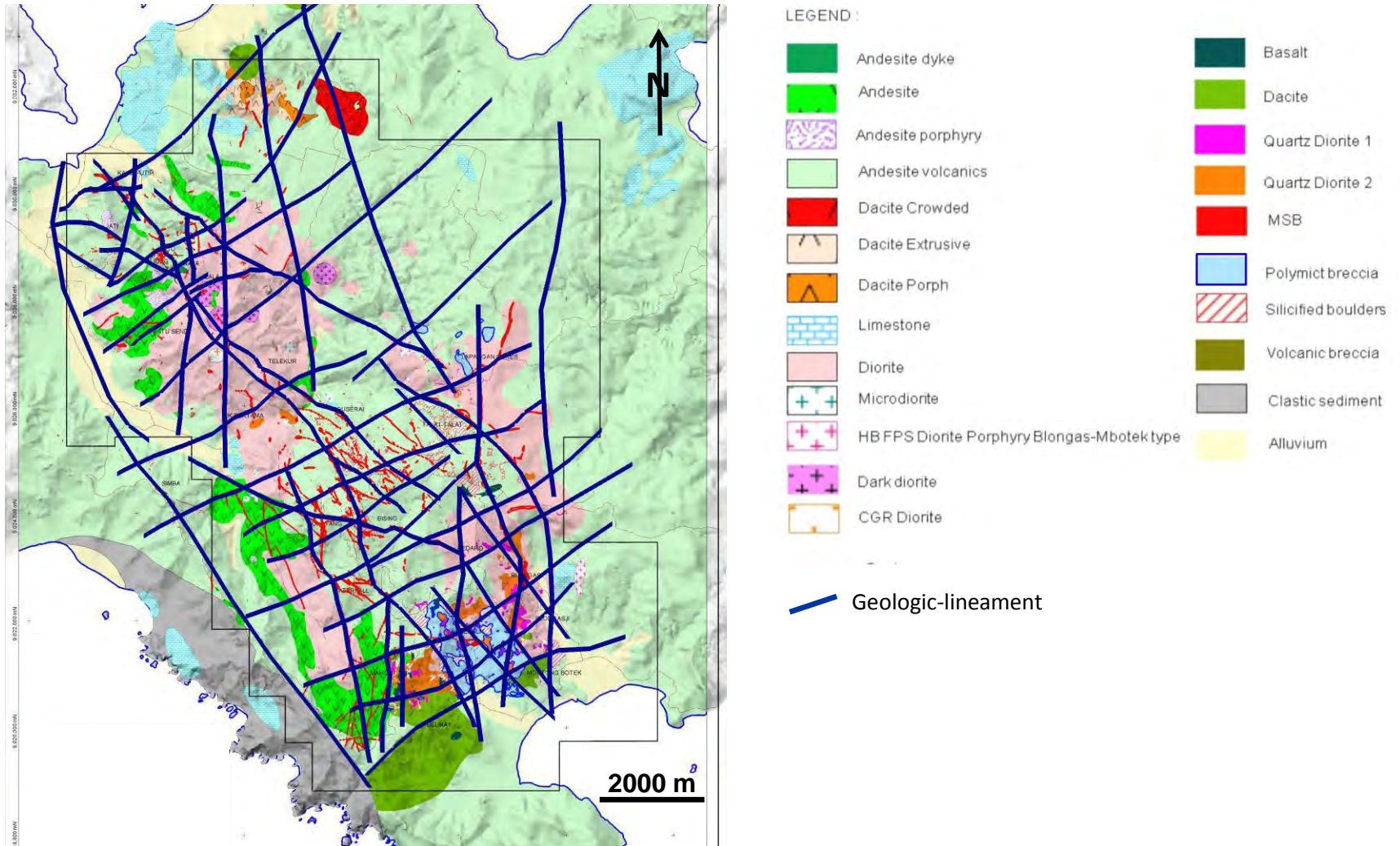


Figure 3: Simplified hydrothermal alteration zones for the SW Lombok IUP of Southern Arc Minerals, incorporating the results of the ongoing regional mapping program. The overlay shows a compilation of structural interpretations made by company geologists and the author.

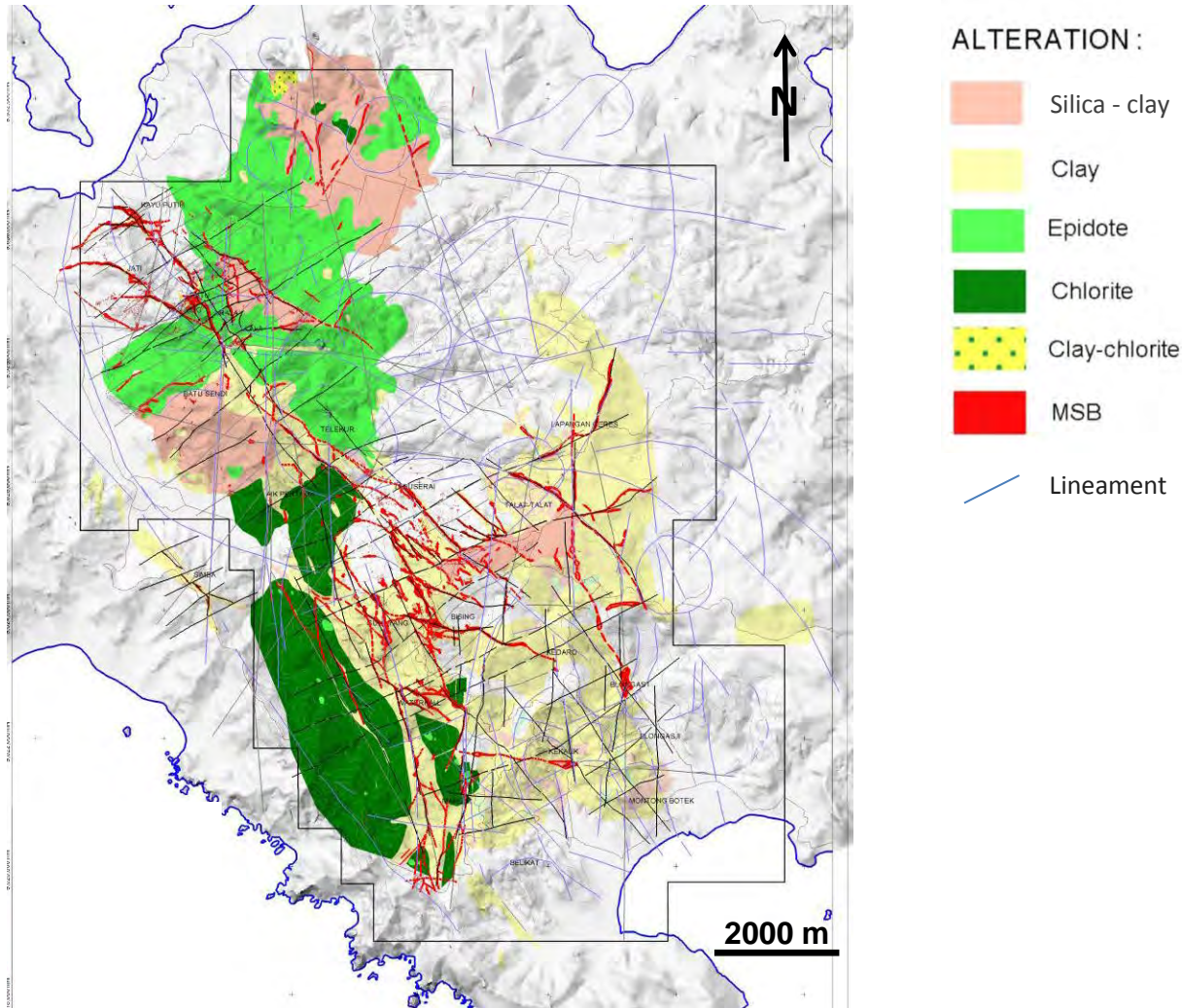


Figure 4: Simplified hydrothermal alteration zones for the SW Lombok IUP of Southern Arc Minerals, incorporating the results of the ongoing regional mapping program and previous structural interpretations. The map shows a geological lineament interpretation based on the distribution of intrusions, quartz-ledges / MSBs and hydrothermal alteration zones. The lineaments (dark blue) are inferred to coincide with deep-seated faults and fracture zones that have guided the emplacement of intrusions and related hydrothermal alteration / mineralization.

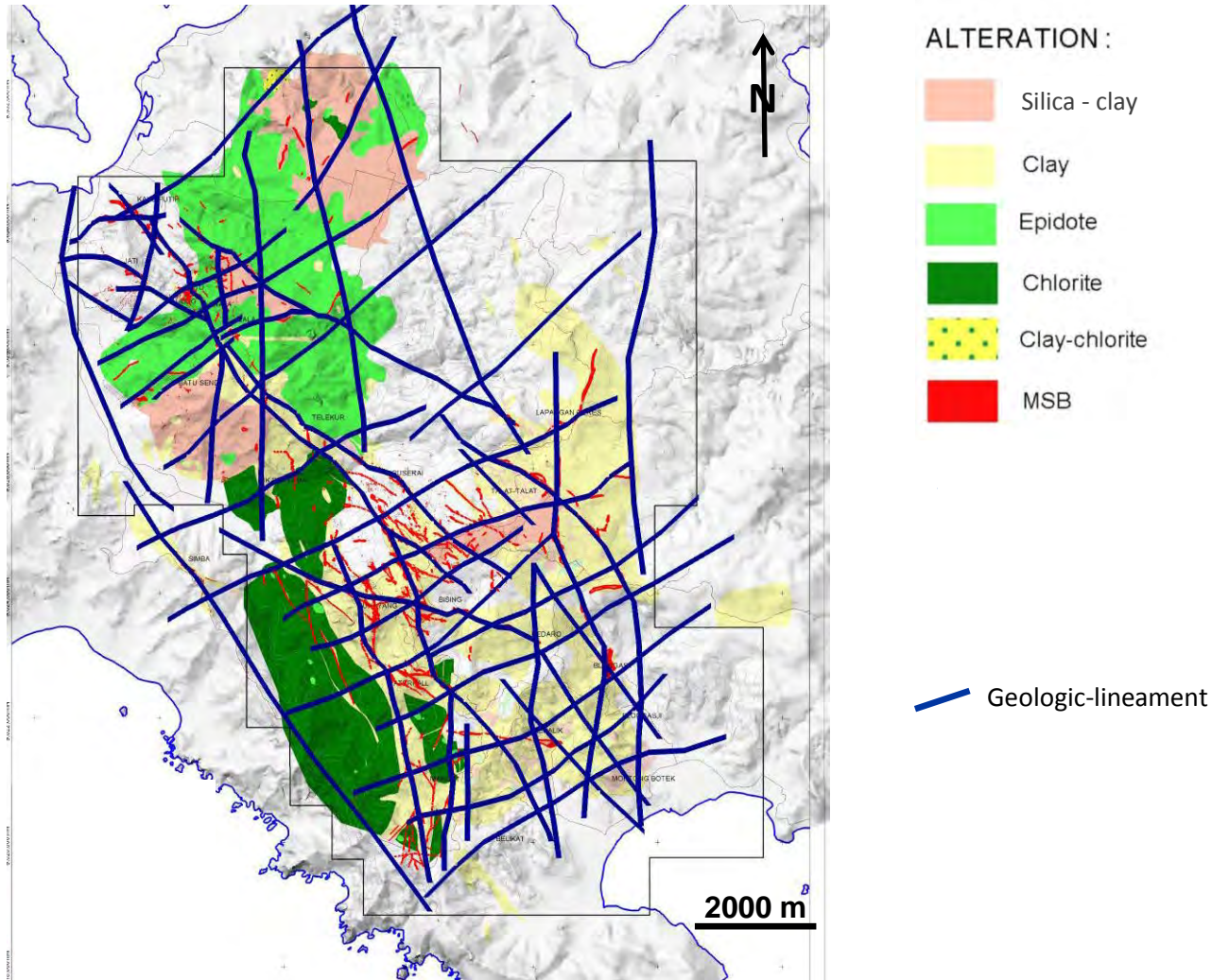
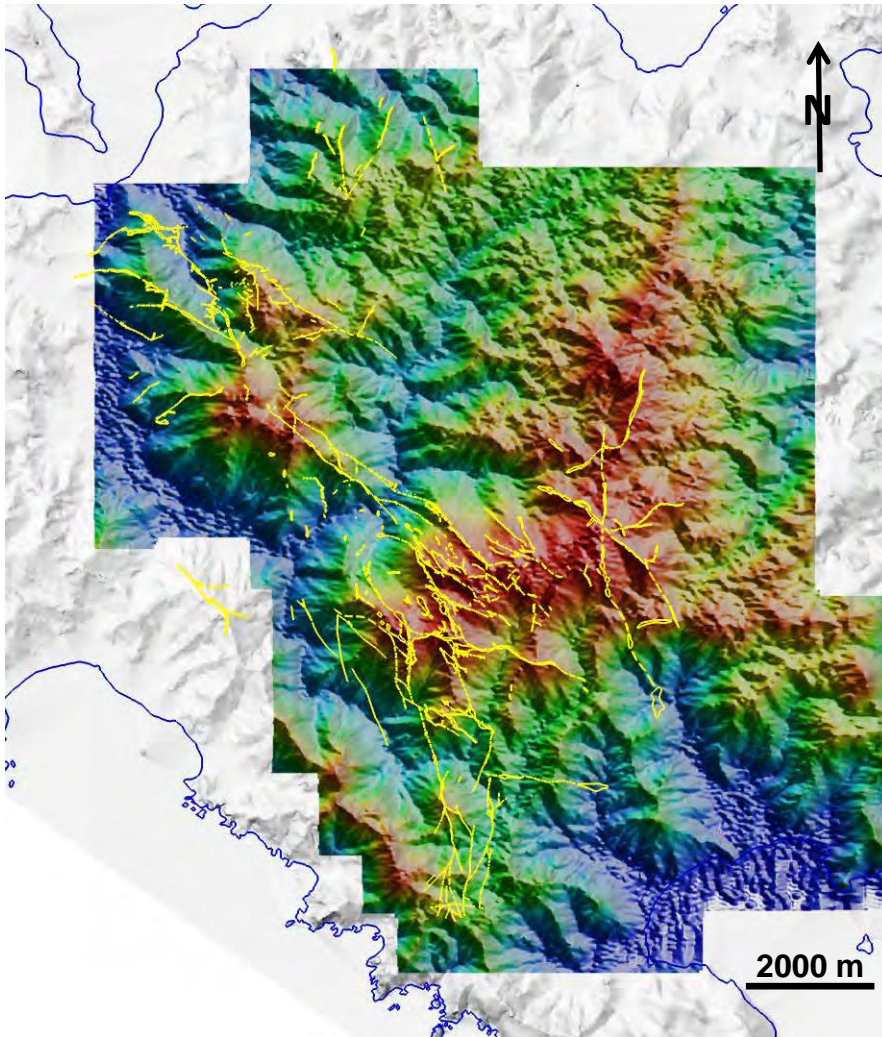
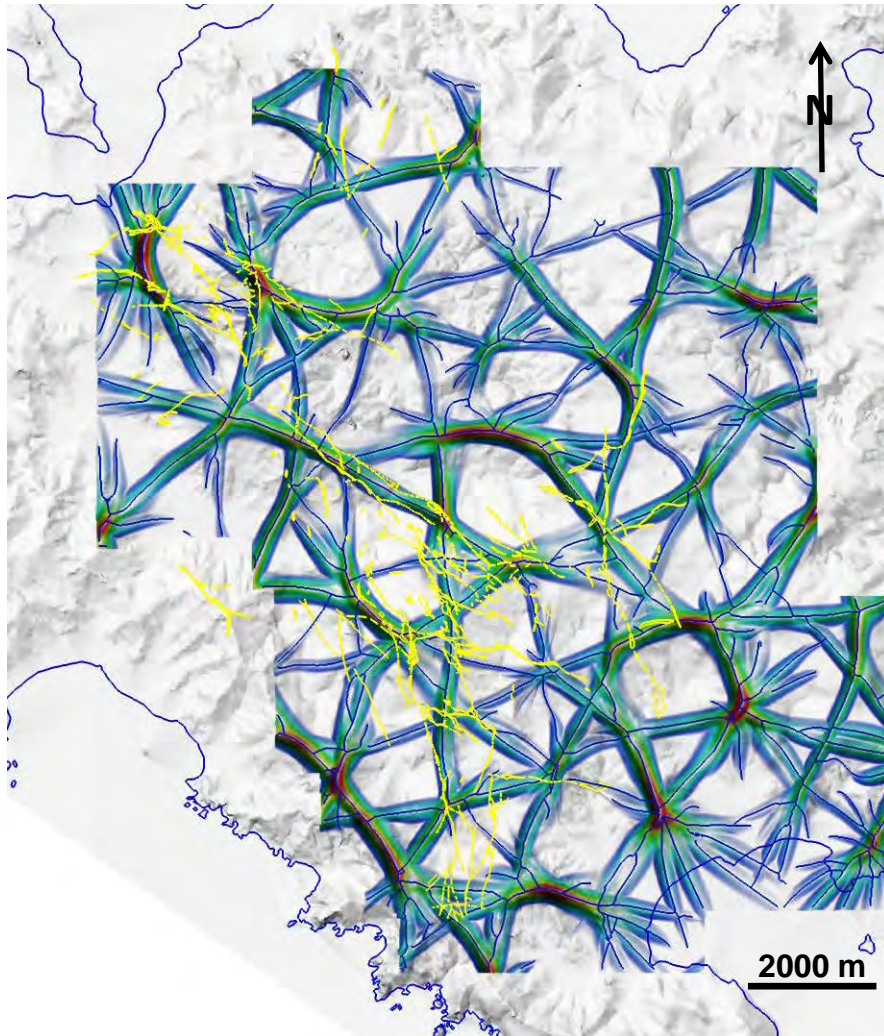


Figure 5: Digital elevation model constructed by Fathom Geophysics (2011) based on radar-altimeter data collected during the recently completed airborne geophysical survey flown by GPX. The overlay shows that many of the quartz-ledges / MSBs (yellow outlines) follow ridge-crests or topographical gradients, which are inferred to be faults or fracture zones.



Butterworth smoothing filter applied
HSI imaging with NE-illumination

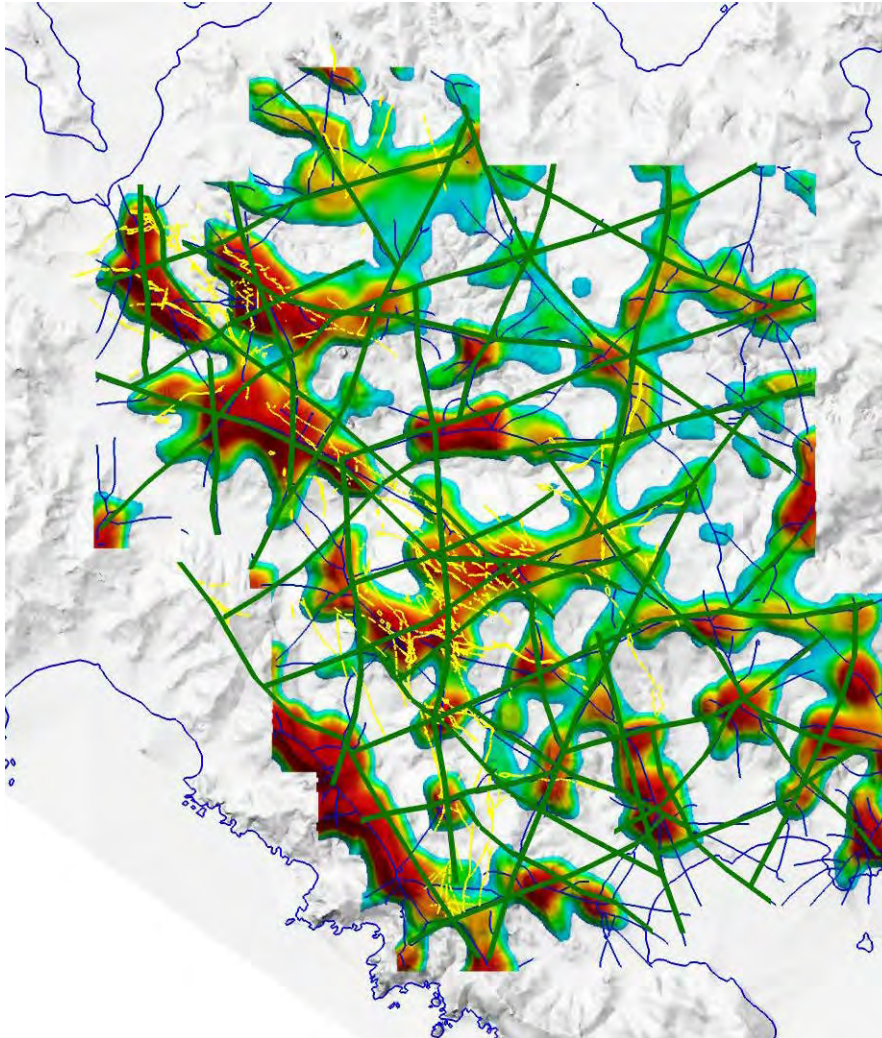
Figure 6: Topographic ridges after applying a 1250 m (low-pass) structure-detection filter to the radar-altimeter topographic data (Fathom Geophysics, 2011) and quartz-ledges / MSBs (yellow outlines). The ridges are color-coded for steepness (blue to red indicates increasing topographic gradient). The overlay shows vectors (dark-blue lines) that coincide with the axes of the large wavelength ridge-crests.



The *structure detection filter* is
An edge detection filter but the
results are significantly different
than those produced by other methods.

The major difference is that the
results are a measure of
asymmetry regardless of
amplitude. This ensures that
structures in areas of low contrast
are highlighted just as well as
those in areas of high contrast.

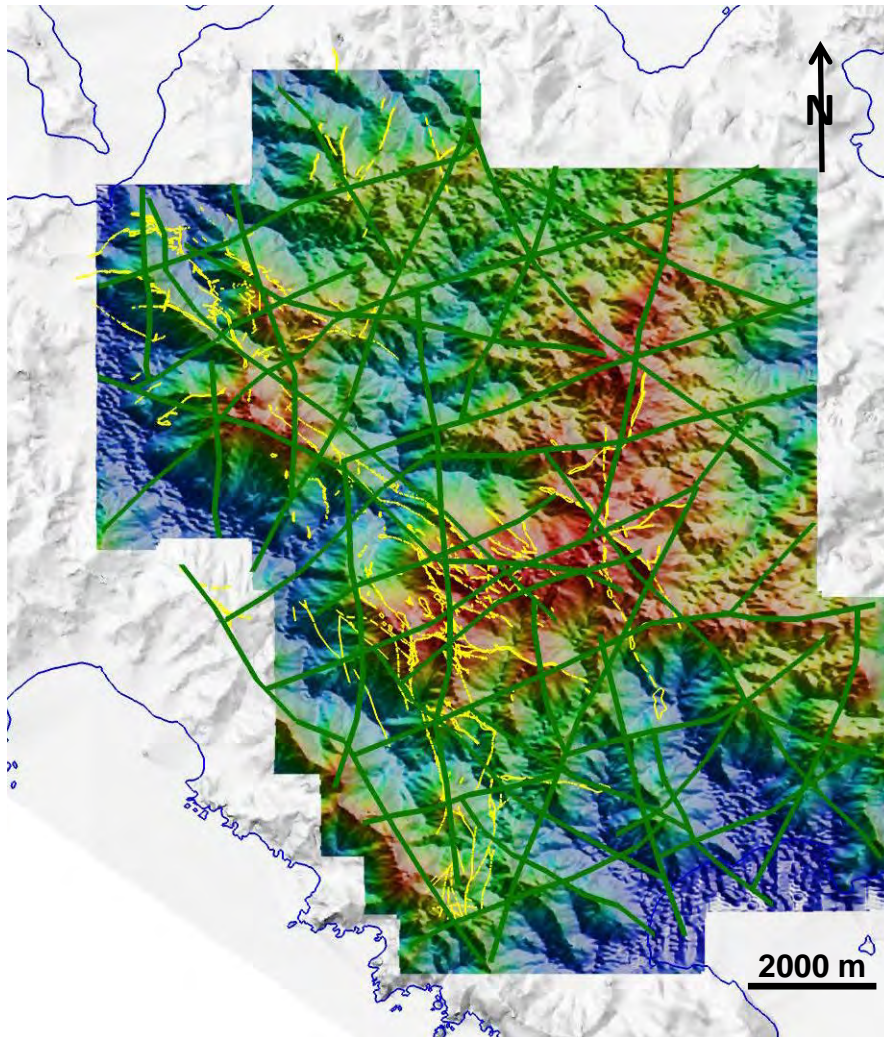
Figure 7: Location of topographic 'horsts' after applying a low-frequency (large-wavelength) top-hat transform to the radar-altimeter topographic data (Fathom Geophysics, 2011) and quartz-ledges / MSBs (yellow outlines). The topographic 'horsts' are color-coded for relative height above the adjacent valleys (cyan to red indicates increasing relative height). The dark-blue lines coincide with the axes of the large wavelength ridge-crests shown in the previous figure. The overlay shows a topographic lineament interpretation (green lines) drawn to coincide with large-wavelength topographic ridge / 'horst' alignment and disruptions in topographic trends.



Top-hat transform: gray-scale morphological operator that extracts the ridges / horsts

— Topographic-lineament

Figure 8: Topographic lineament interpretation (green lines) and quartz-ledges / MSBs (yellow outlines) shown on the HSI image of the digital elevation model.



Butterworth smoothing filter applied
HSI imaging with NE-illumination


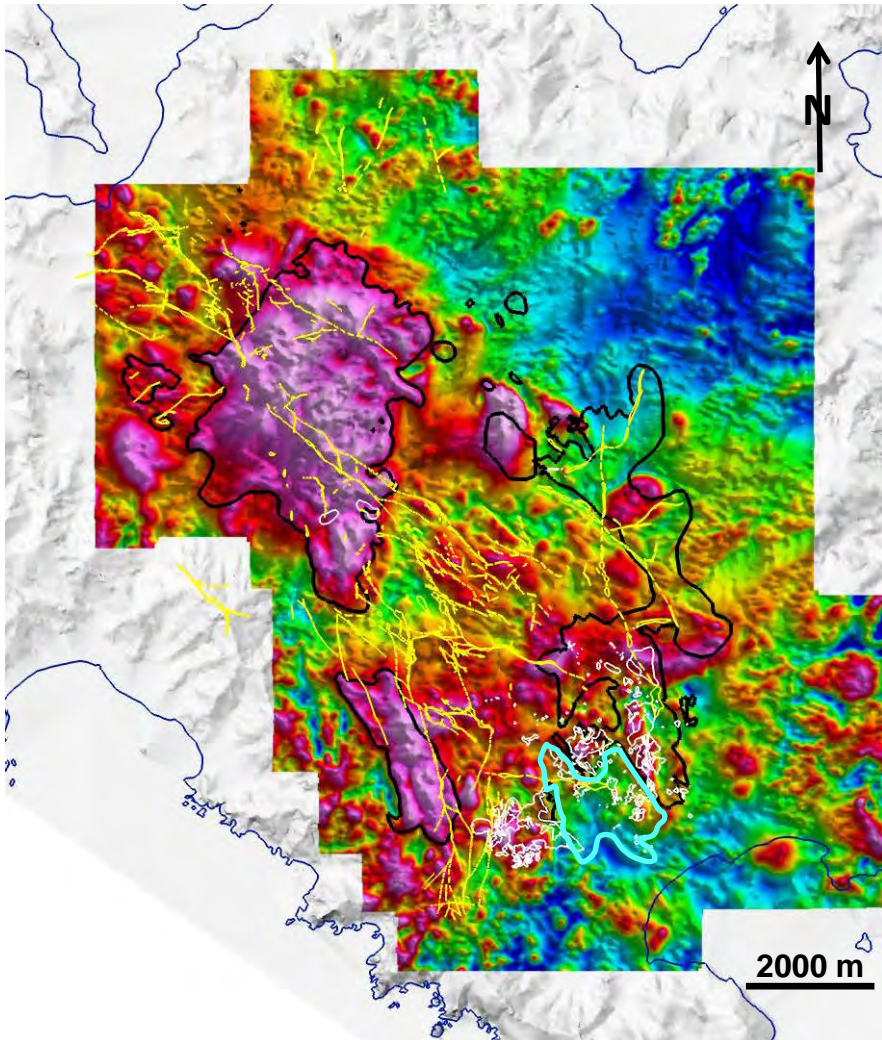
 Topographic-lineament

Figure 9: Reduced to the pole magnetics as processed by Fathom Geophysics (2011) from data collected by GPX during the recently completed airborne geophysical survey. The overlay shows that the equigranular diorite plutons (black outline) coincide with portions of the large magnetic highs. quartz diorites (white outlines), which are associated with magnetite-stable potassic and intermediate argillic alteration in Selodong, are expressed by discrete magnetic highs. The polymictic breccia (cyan outline), which is characterized by magnetite-destructive quartz-clay-pyrite alteration, coincides with a relative magnetic low that forms an embayment to the large magnetic high in Selodong. Many of the quartz-ledges / MSBs (yellow outlines) coincide with magnetic gradients, which are inferred to be faults or fracture zones.



Histogram equalized colour-stretch

Figure 10: Pseudo-gravity image of the reduced to the pole magnetic data for the 0 – 1000 m residual as processed by Fathom Geophysics (2011). Several of the quartz-ledges / MSBs (yellow outlines) coincide with magnetic gradients, which are inferred to be faults or fracture zones.

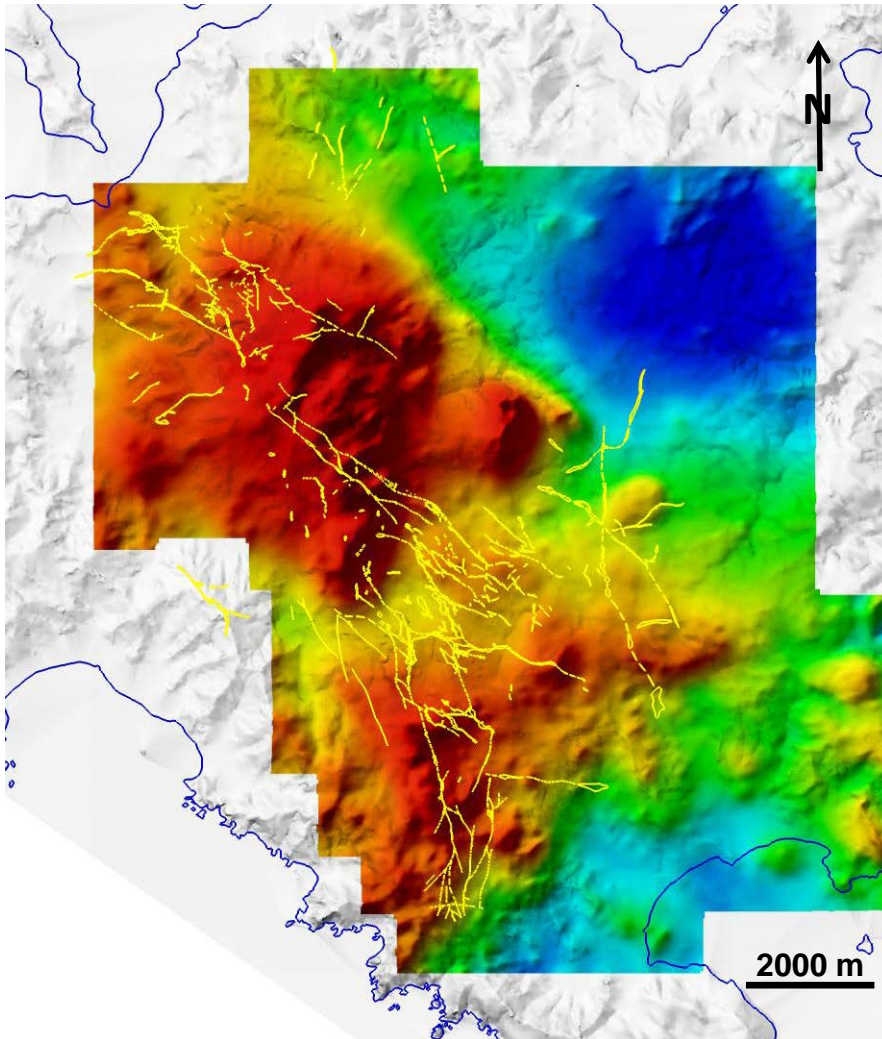


Figure 11: Deep residual of the reduced to the pole magnetics after the application of a 250 – 1000 m band-pass filter by Fathom Geophysics (2011). The black polygons in the overlay represent high-level magnetic highs with radial-symmetry (400 m search diameter) that coincide with mid-level magnetic highs (1 km search diameter) *and* lie above, or within 1 km of, deep-level magnetic highs (2.5 km search diameter). These ‘connected’ high-level magnetic highs are inferred to be candidates for near-surface magnetic stocks (e.g., diorite) or cupolas above potential porphyry systems.

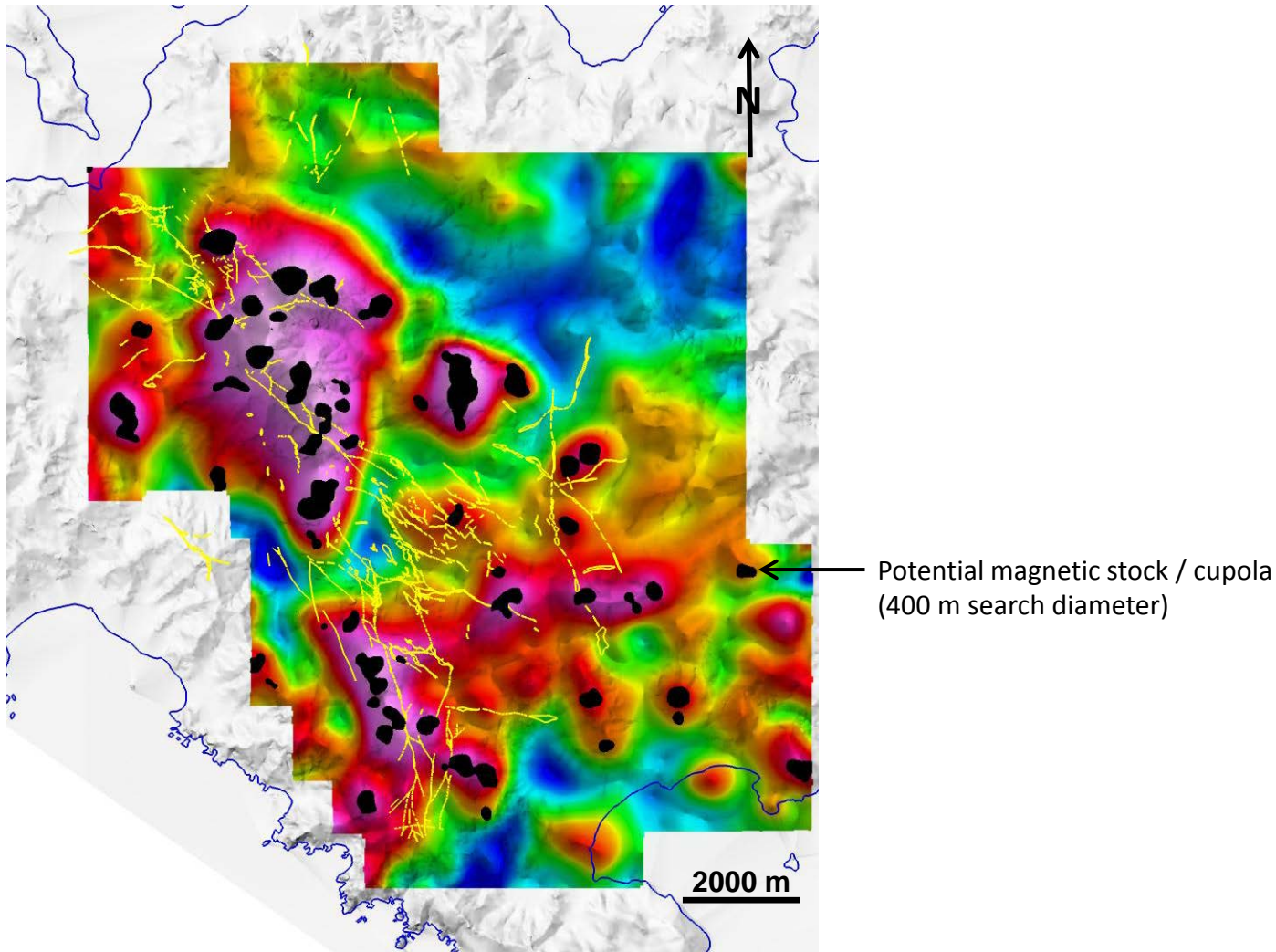
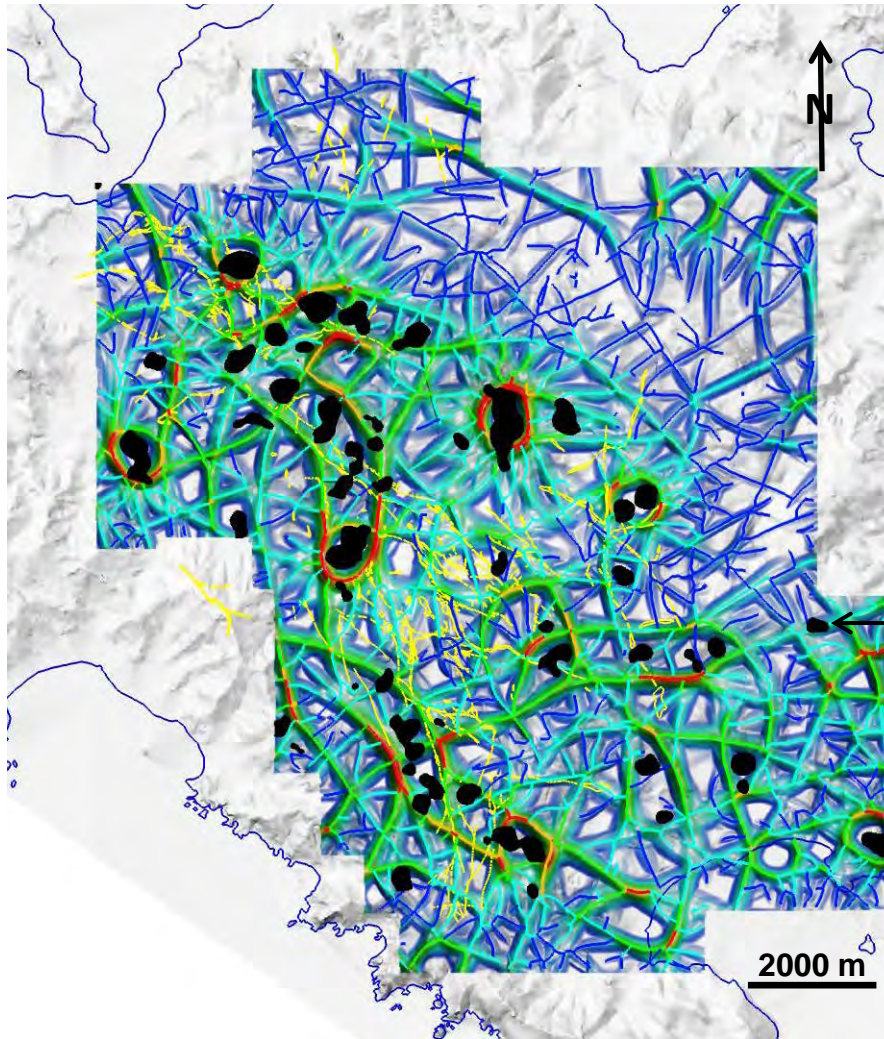


Figure 12: Deep magnetic gradients / edges after applying a 1250 m (low-pass) structure-detection filter to the reduced to the pole magnetic data by Fathom Geophysics (2011). The magnetic gradients are color-coded; blue to red indicates increasing magnetic gradient. The black polygons indicate high-level magnetic highs with radial-symmetry that are connected to mid- and deep-level magnetic highs and inferred to be related to near-surface magnetic stocks (e.g., diorite) or cupolas above potential porphyry systems.



The *structure detection filter* is
An edge detection filter but the
results are significantly different
than those produced by other methods.

The major difference is that the
results are a measure of
asymmetry regardless of
amplitude. This ensures that
structures in areas of low contrast
are highlighted just as well as
those in areas of high contrast.

Potential magnetic stock / cupola
(400 m search diameter)

Figure 13: Deep residual (250 – 1000 m) of the reduced to the pole magnetics, deep magnetic gradients (blue to red for increasing gradient) and high-level magnetic highs (black polygons) with radial-symmetry that are connected to mid- and deep-level magnetic highs and inferred to be related to near-surface magnetic stocks (e.g., diorite) or cupolas above potential porphyry systems.

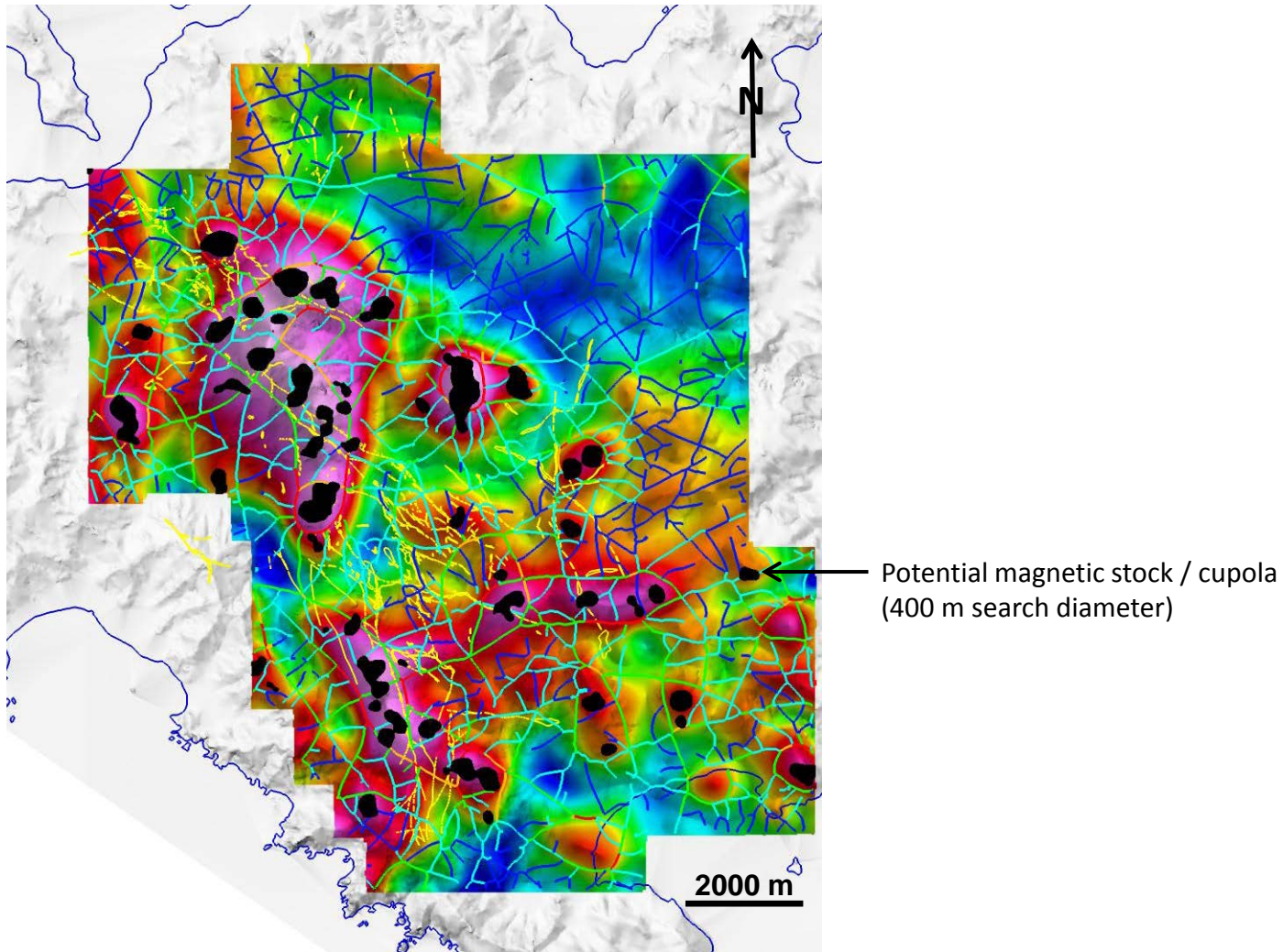
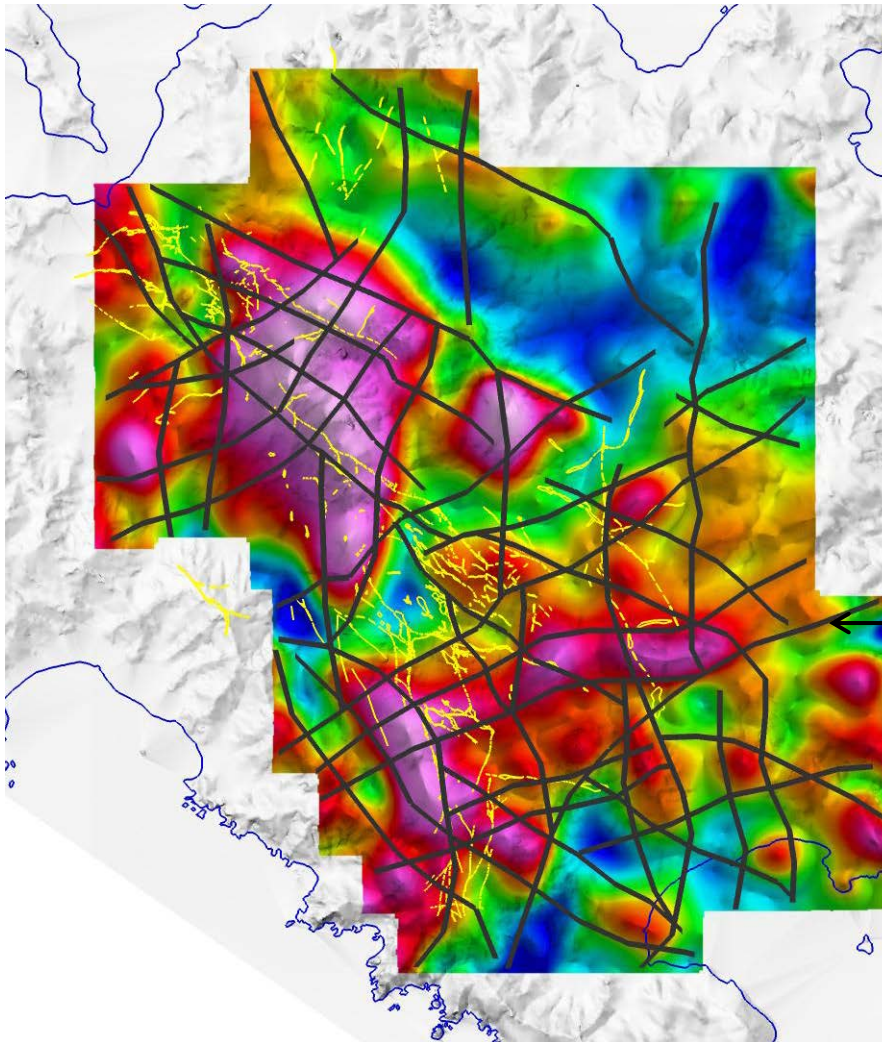


Figure 14: Magnetic lineament interpretation (dark-grey lines) and quartz-ledges / MSBs (yellow outlines) shown on deep residual of the reduced to the pole magnetics and deep magnetic gradients. The black polygons represent 'connected' high-level magnetic highs that are inferred to be related to near-surface magnetic stocks (e.g., diorite) or cupolas above potential porphyry systems. The magnetic lineaments are drawn to coincide with deep magnetic gradients and the distribution of the high-level magnetic highs that are connected to larger magnetic highs at depth. The overlay shows the magnetic lineaments and quartz-ledges / MSBs on top of the deep residual reduced to the pole magnetic image.



— Magnetic-lineament

Figure 15: Geologic-, topographic- and magnetic-lineaments shown on simplified geology for the SW Lombok IUP. There is a good spatial coincidence of lineaments, which suggests that the geology influences the topography and magnetic expression of the area.

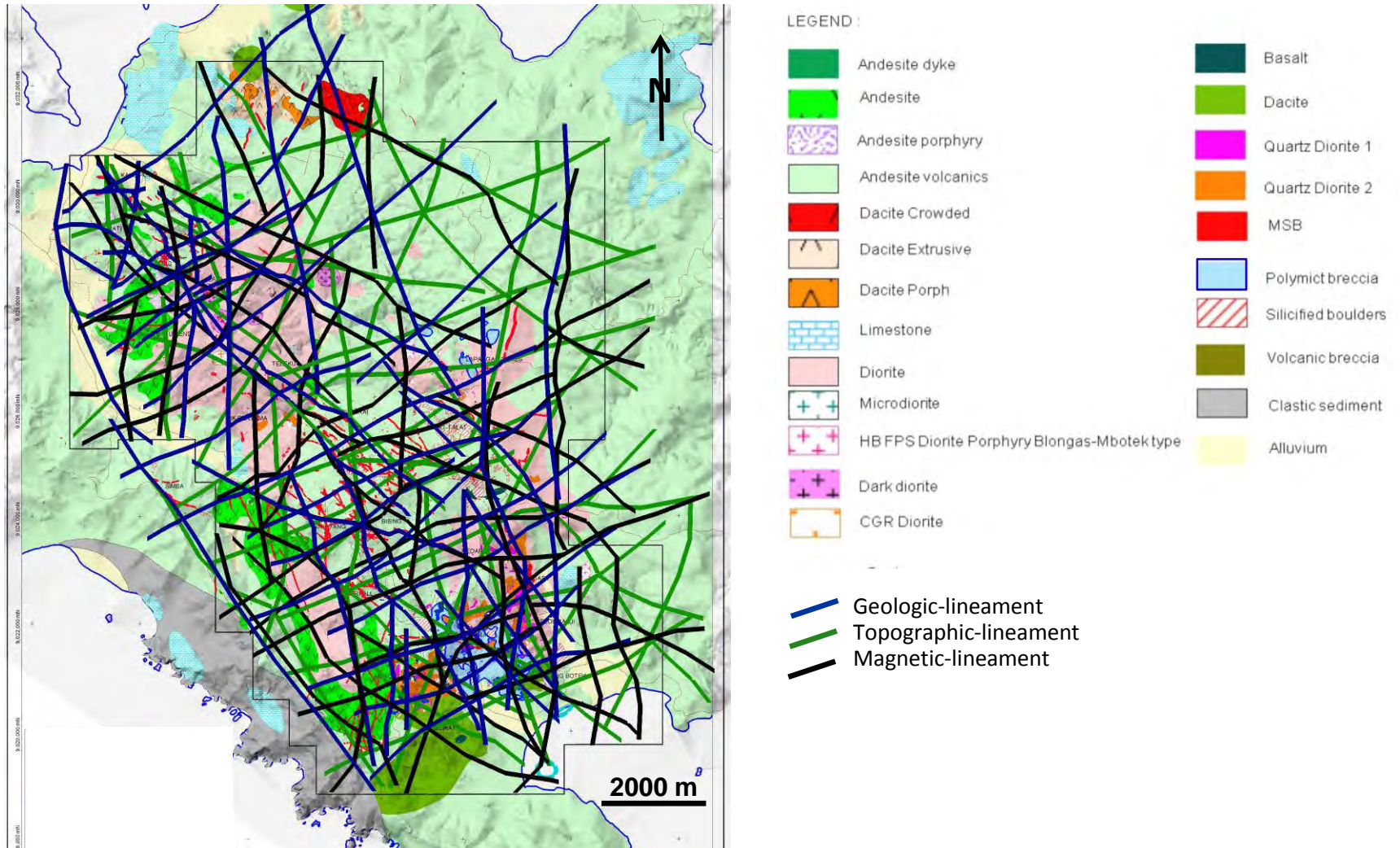


Figure 16: Combined lineaments shown on simplified geology for the SW Lombok IUP. Zones of increased lineament abundance and lineament intersections are inferred to indicate favourable pathways for ascending magmas and hydrothermal fluids. The overlay shows the density contours for the combined lineaments (blue to red for increasing lineament density). The density contours are used as a way to score the prospectivity of the SW Lombok IUP with regards to potential pathways for porphyry-related mineralization. The relationship of the pathway scores to lithology and hydrothermal alteration are illustrated in the subsequent figures.

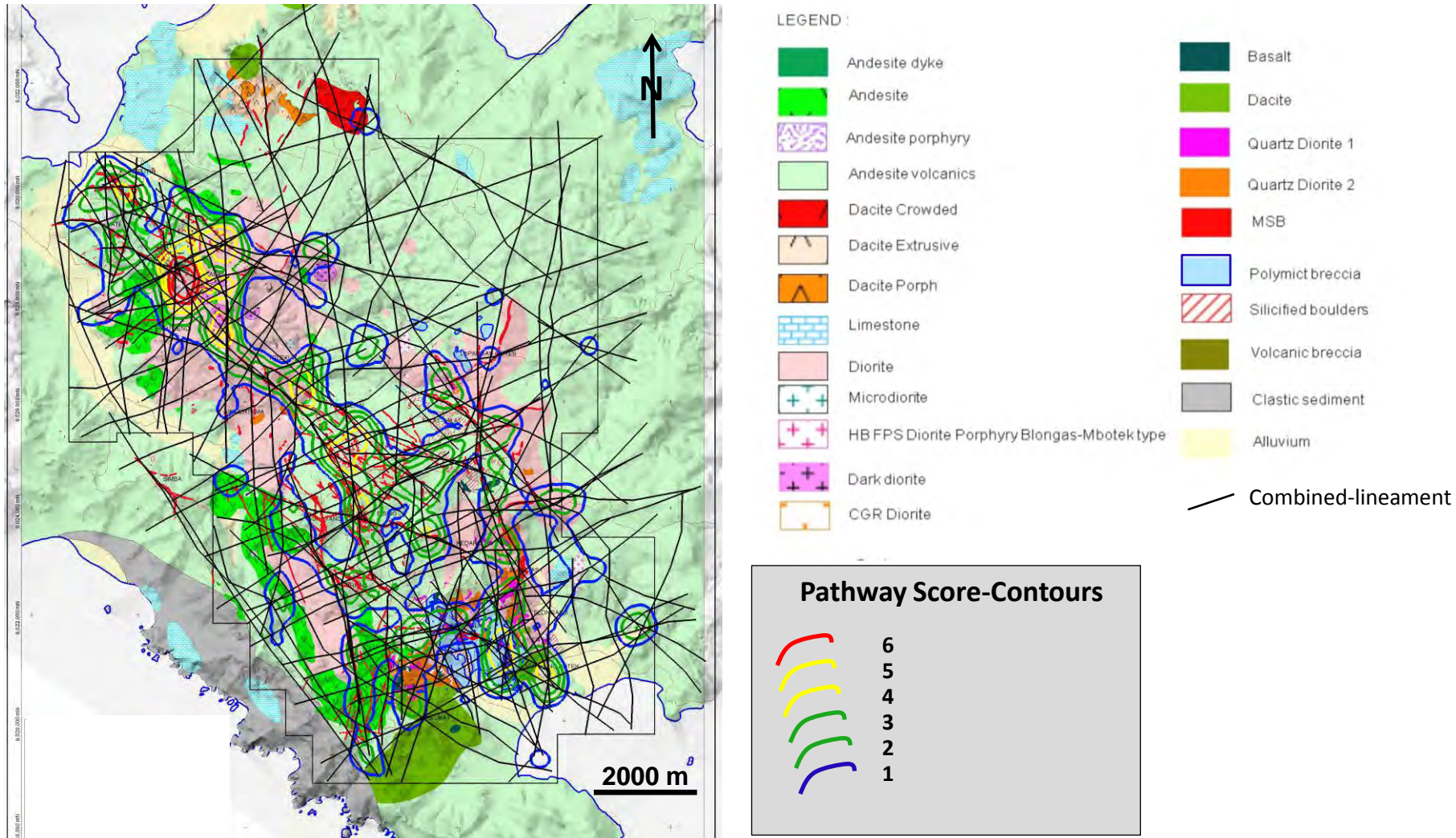
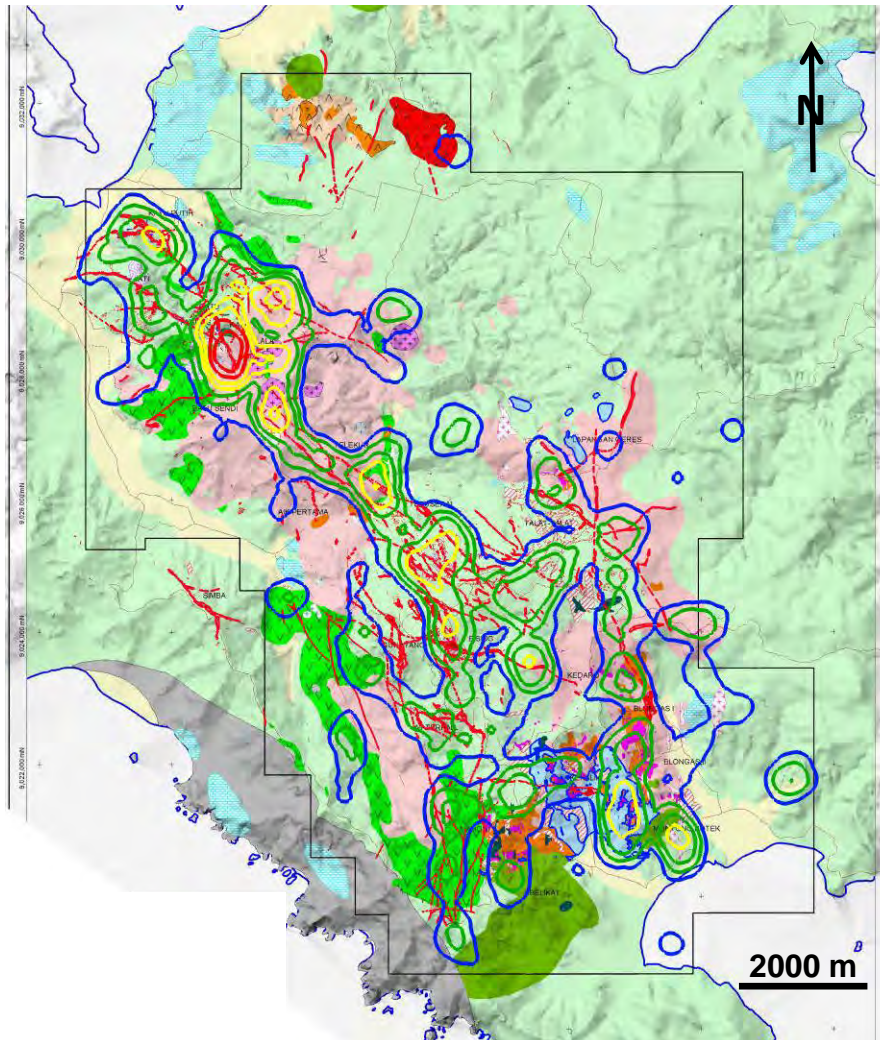


Figure 17: Combined lineament density contours / pathway scores (blue to red indicates increasing score) shown on simplified geology for the SW Lombok IUP. Zones of increased lineament abundance and lineament intersections are inferred to indicate favourable pathways for ascending magmas and hydrothermal fluids. Zones of increased lineament density coincide with the major quartz-ledge / MSB trends, quartz diorites and the margins of equigranular diorite plutons.



LEGEND :

- | | | | |
|---|---|---|---------------------|
|  | Andesite dyke |  | Basalt |
|  | Andesite |  | Dacite |
|  | Andesite porphyry |  | Quartz Diorite 1 |
|  | Andesite volcanics |  | Quartz Diorite 2 |
|  | Dacite Crowded |  | MSB |
|  | Dacite Extrusive |  | Polymict breccia |
|  | Dacite Porph |  | Silicified boulders |
|  | Limestone |  | Volcanic breccia |
|  | Diorite |  | Clastic sediment |
|  | Microdiorite |  | Alluvium |
|  | HB FPS Diorite Porphyry Blongas-Mbotek type | | |
|  | Dark diorite | | |
|  | CGR Diorite | | |

Pathway Score-Contours



6

5

4

3

2

1

Figure 18: Combined lineament density contours / pathway scores (blue to red indicates increasing score) shown on simplified hydrothermal alteration for the SW Lombok IUP. Zones of increased lineament abundance and lineament intersections are inferred to indicate favourable pathways for ascending magmas and hydrothermal fluids. Zones of increased lineament density coincide with the major quartz-ledge / MSB trends, clay- alteration and locally, silica-clay alteration zones.

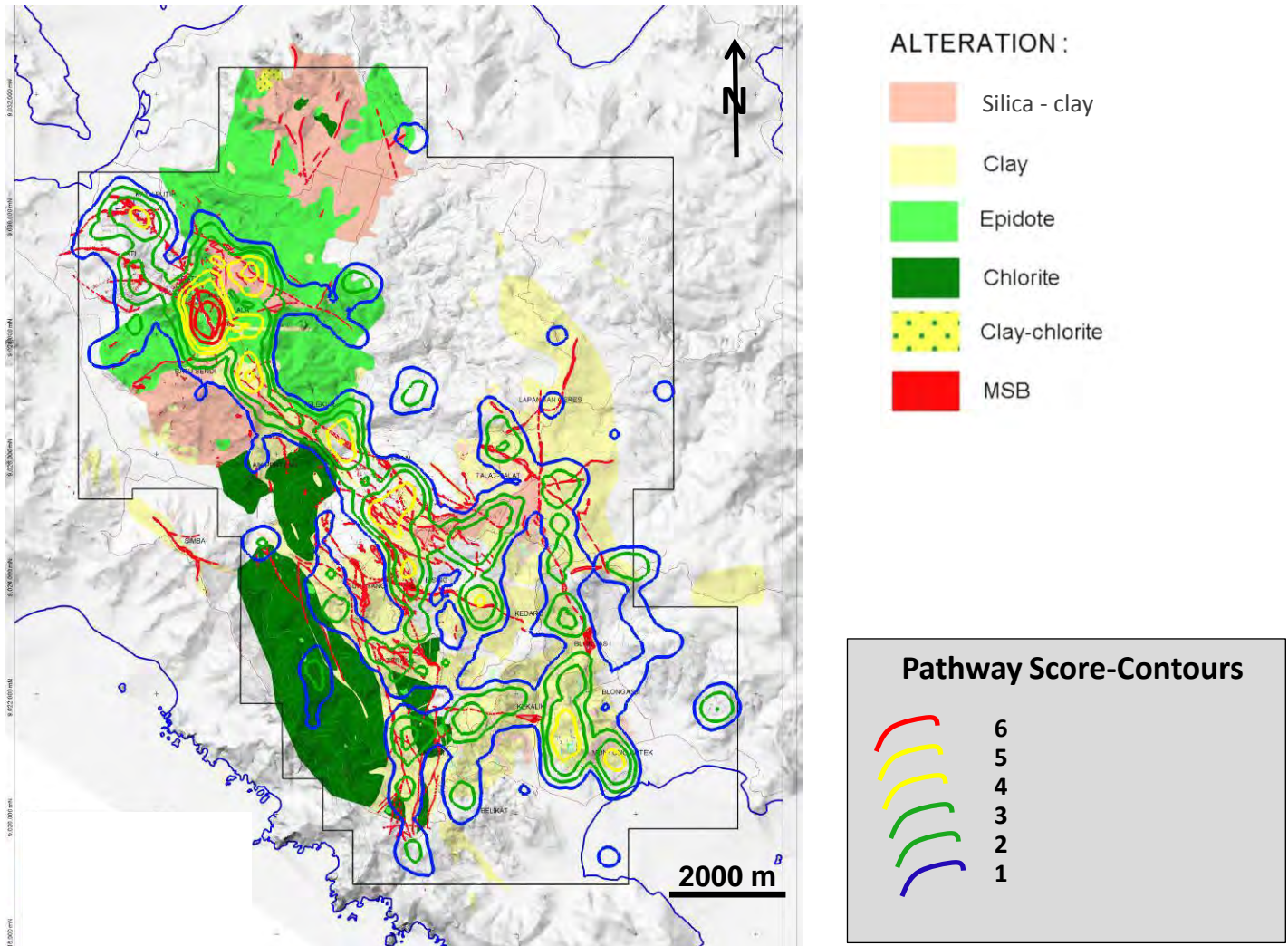


Figure 19: Distribution of equigranular diorite plutons (pink) and quartz diorite and dacite porphyries (dark-red) shown on simplified geology for the SW Lombok IUP. The interpreted diorite contact is inferred to act as a focus for porphyritic- and felsic-stocks that are associated with porphyry-style mineralization at Selodong. The overlay shows a 500 m buffer to the diorite margin, which is inferred to indicate a prospective zone for potential porphyry systems in the SW Lombok IUP.

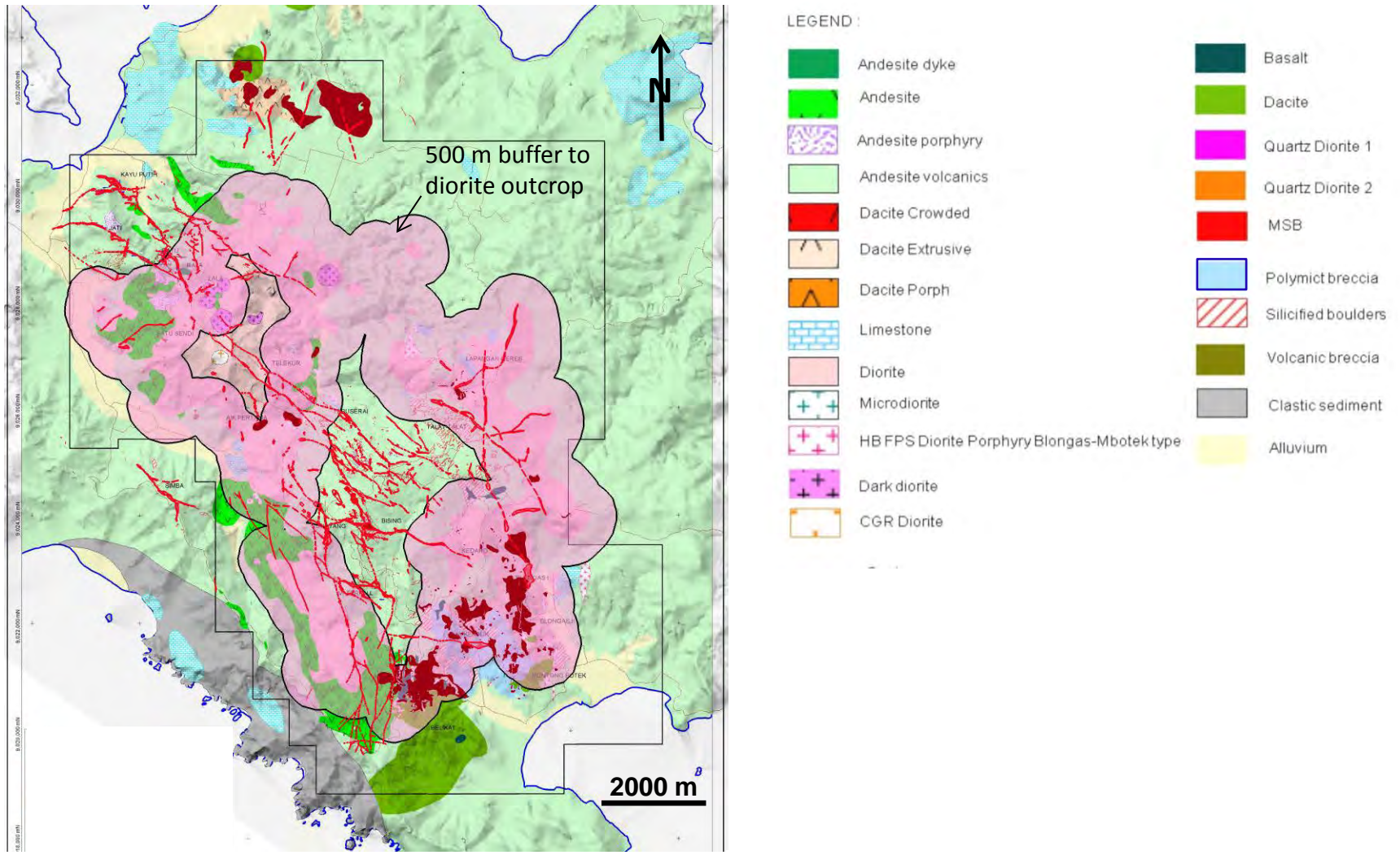


Figure 20: Distribution of silica-clay alteration zones (purple polygons) shown on simplified hydrothermal alteration for the SW Lombok IUP. The silica-clay-rich zones are inferred to indicate areas of focused hydrothermal fluid-flow. Spectral (SWIR) analyses show that the silica-clay zones in Mencanggih and the northern part of Batu Sendi contain variable amounts of dickite, alunite and pyrophyllite, which indicate a high-temperature advanced argillic (low pH) alteration assemblage (pyrophyllite is stable above 300°C). The Lala silica-clay zone contains kaolinite, dickite and alunite, which indicates advanced argillic alteration < 300°C. The southern part of Batu Sendi and Sundancer are characterized by illite and minor paragonite, which indicates near-neutral pH conditions.

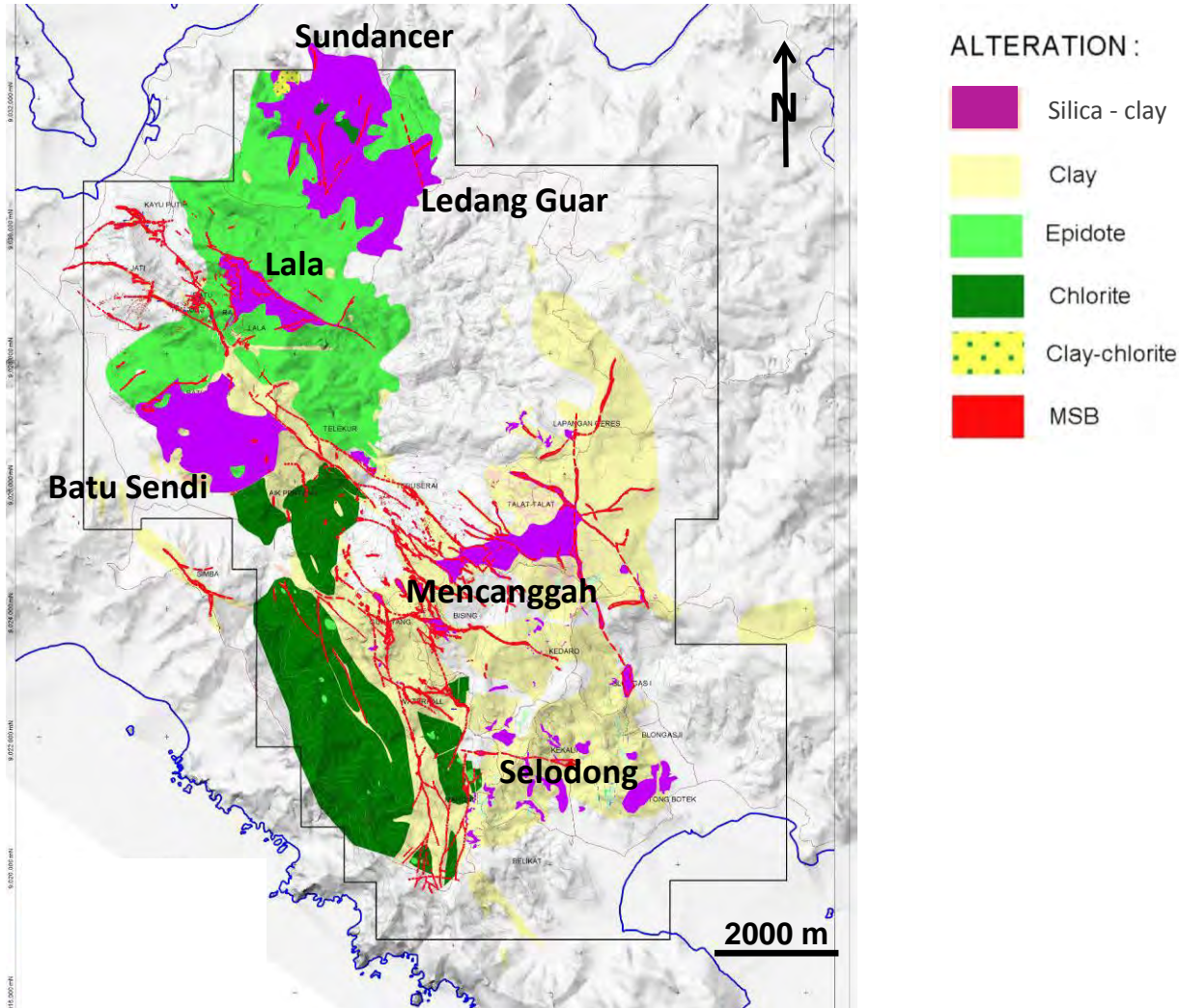


Figure 21: Quartz-ledges / MSBs (yellow outlines) and radiometric K/Th results from the recently completed airborne geophysical survey in the SW Lombok IUP. The silica-clay alteration zones (transparent purple polygons in the overlay) indicate the loss of potassium (low K/Th) in the Mencanggih and Batu Sendi areas, which are characterized by advanced argillic alteration. The silica-clay zones at Selodong, Lala and Ledang Guar display moderate to weak potassium -depletion. The Sundancer silica-clay zone is characterized by high k/Th. The black outlines indicate zones of intense advanced argillic alteration and potassium depletion, which are inferred to be the expression of focused hydrothermal fluid flow above potential porphyry systems. The Mencanggih and Batu Sendi advanced argillic zones are inferred to represent potential lithocaps to concealed porphyry systems.

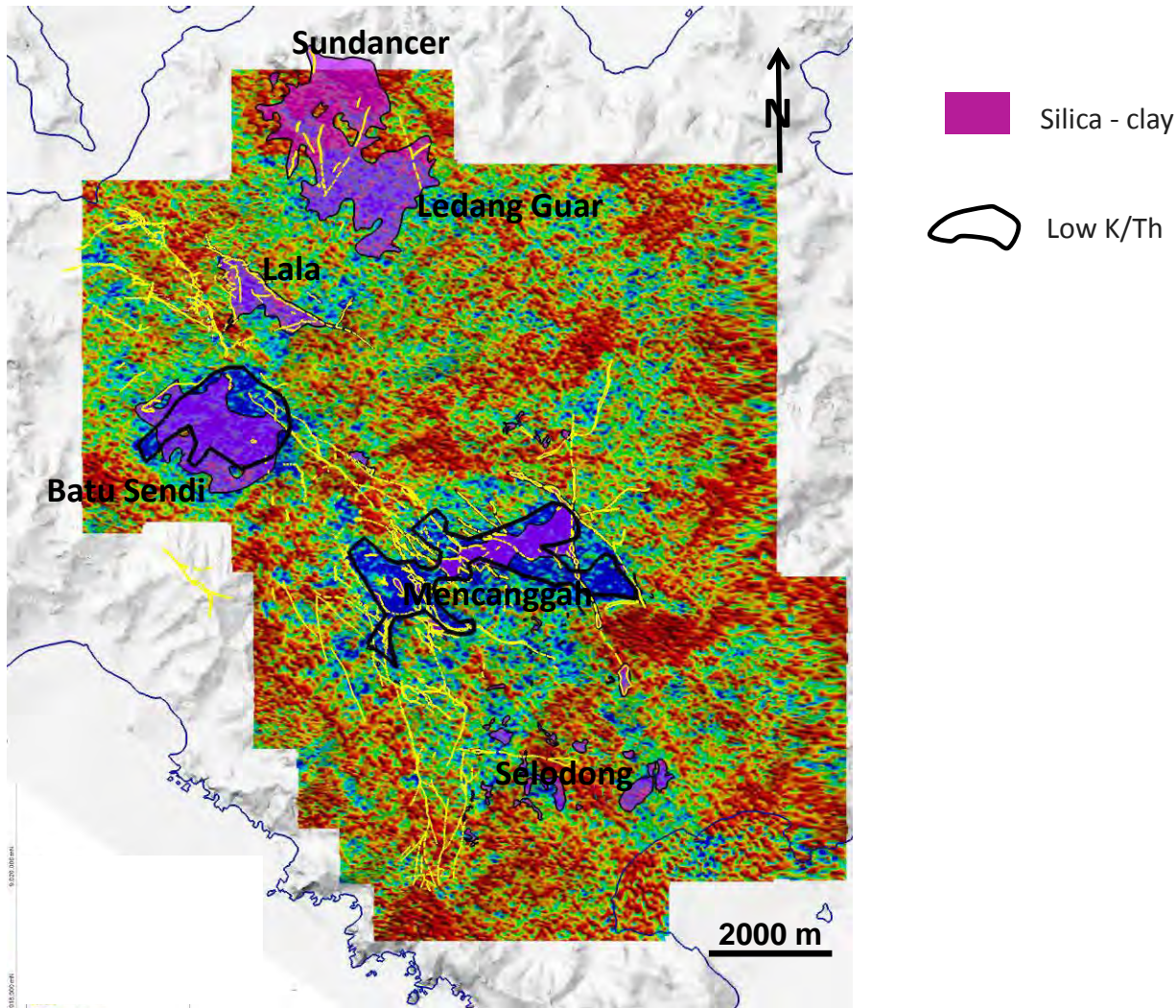


Figure 22: Deep-level magnetic highs that exhibit radial-symmetry (2.5 km search diameter), which are inferred to represent equigranular diorite plutons near-surface and at depth. The surface distribution of equigranular diorite mostly coincides with the deep-level magnetic bodies. The quartz diorite porphyries in the Selodong area lie adjacent to the margins and within the outline of the deep-level magnetic high. The polymictic breccia (orange outline), which is characterized by magnetite-destructive quartz-clay-pyrite alteration, sits in the embayment to the large magnetic high in Selodong. The margins of the deep magnetic highs are buffered by 1000 m to indicate potential focus-zones for porphyry deposit emplacement. The quartz-ledges / MSBs (yellow outlines) are shown for geographical reference.

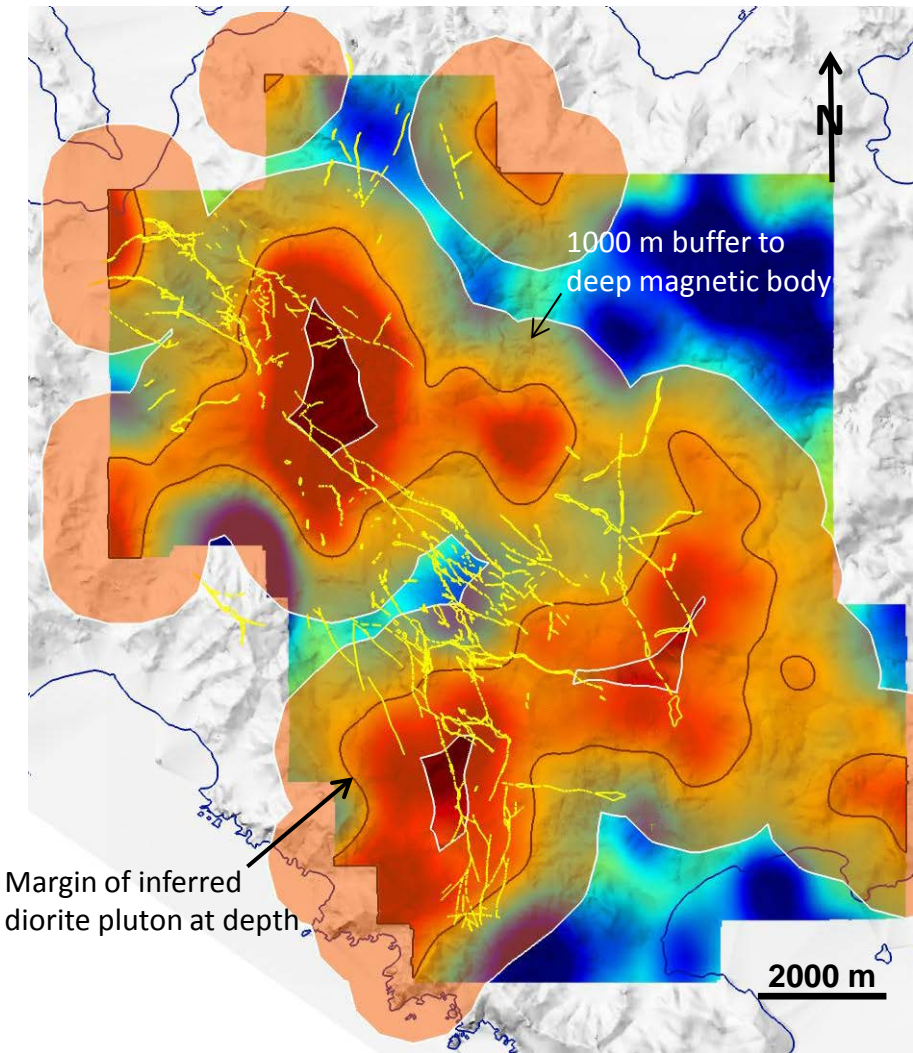


Figure 23: High-level 'connected' magnetic-highs with radial-symmetry (black polygons), which indicate potential stocks and cupolas, shown on a base map of deep-level magnetic-highs / inferred plutons. The potential magnetic stocks or cupolas that lie within 1000 m of the margin of the deep-level plutons indicate potential sites for porphyry deposit emplacement. The quartz-ledges / MSBs (yellow outlines) are shown for geographical reference.

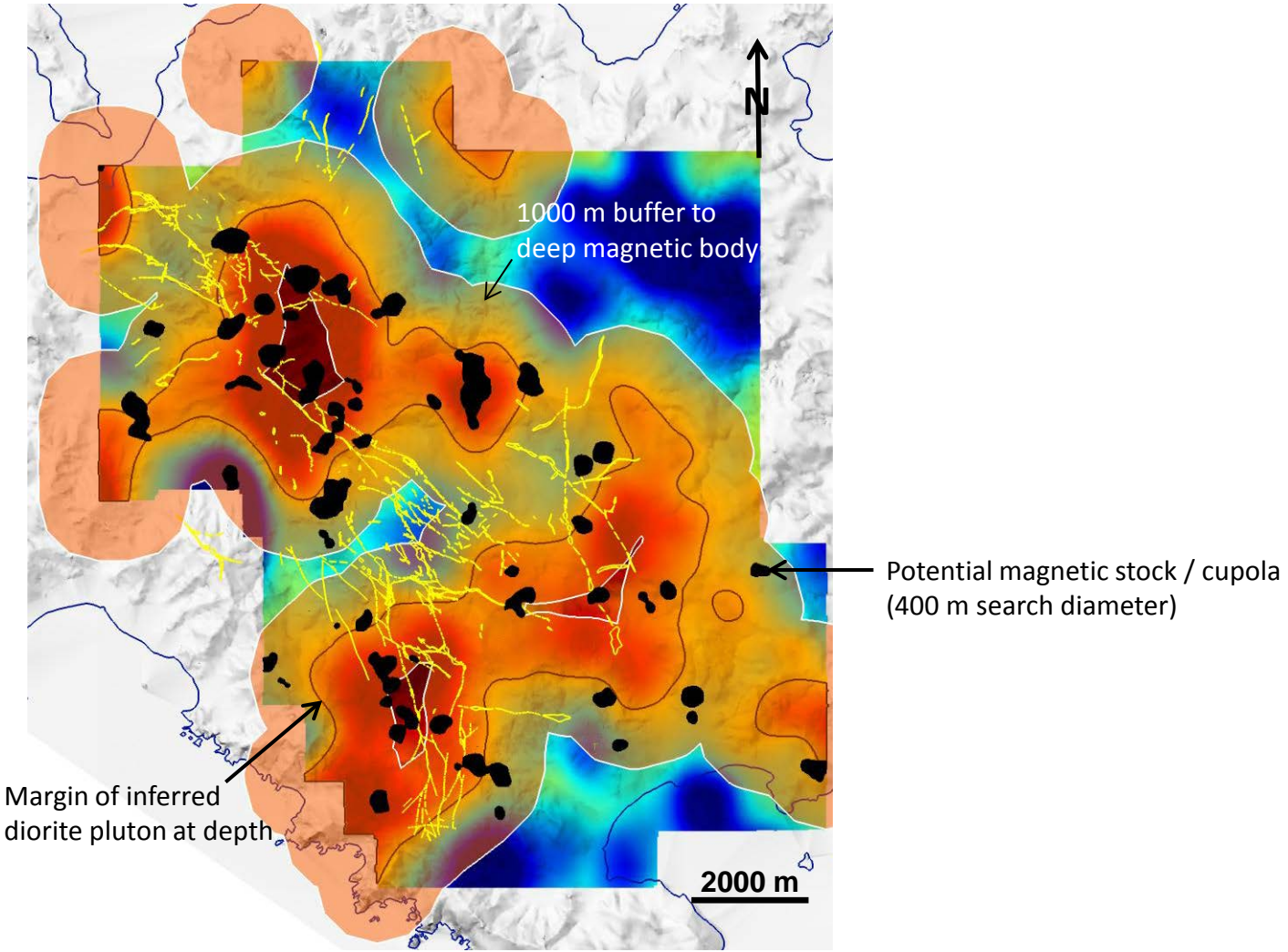


Figure 24: Focus-scores shown on simplified geology for the SW Lombok IUP. The scores are derived by color-coding the number of overlapping polygons created from the superimposition of the favourable geological, hydrothermal alteration and magnetic relationships presented in Figures 19 to 23. The greater the number of overlapping features indicates the higher the probability for the focusing of ascending magma and the development of a porphyry-system. The focus-scores are indicated by cyan (two overlaps), green (three overlaps), yellow (four overlaps) and red (five overlaps out of a possible six). The overlay shows the result of gridding the focus polygons using the minimum-curvature method in the surface grid tools available in Discover version 12.0. The focus-prospectivity grid is scored from moderate-prospectivity (cyan) to high-prospectivity (red).

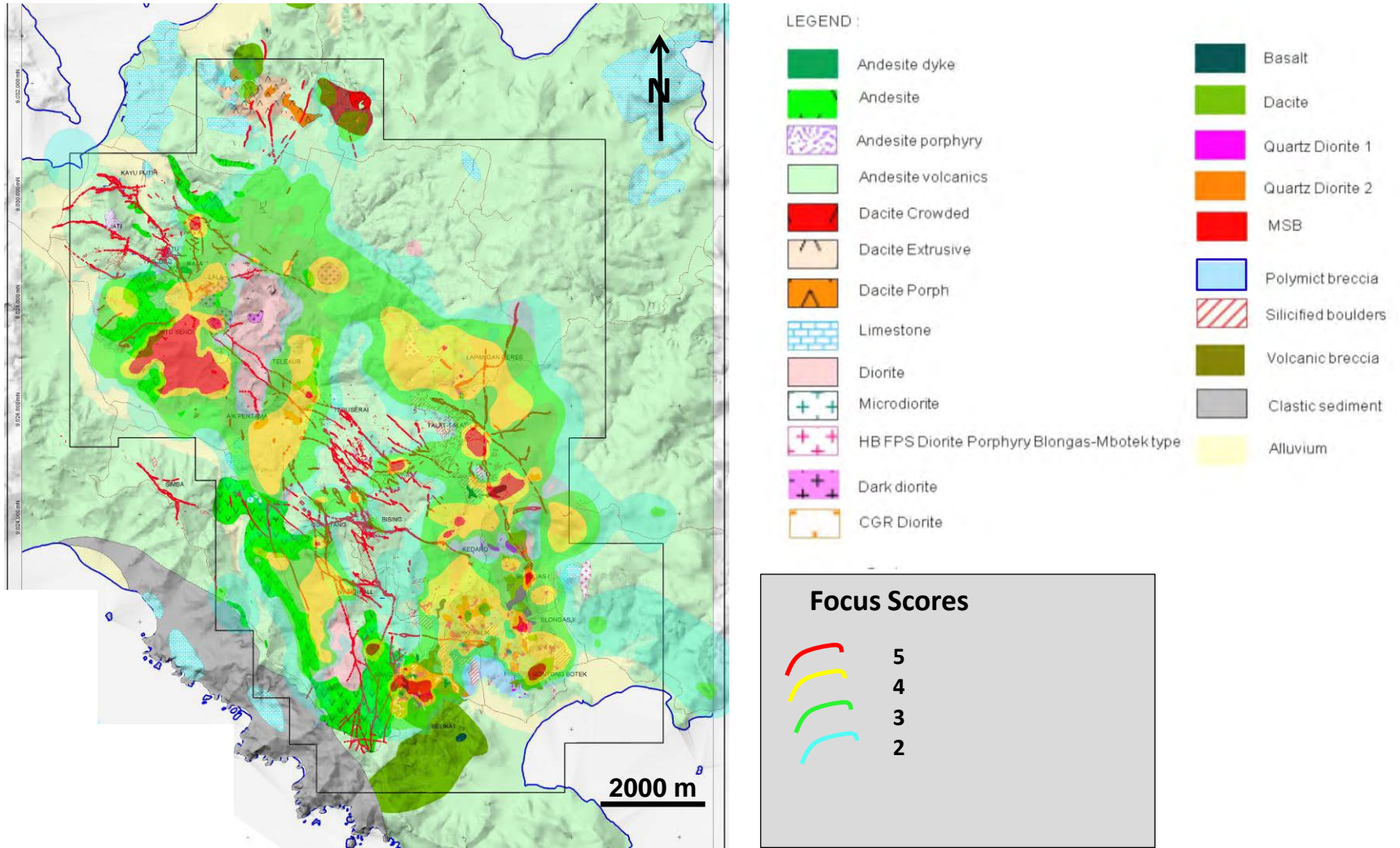


Figure 25: Focus-scores shown on simplified hydrothermal alteration for the SW Lombok IUP. The scores are derived by color-coding the number of overlapping polygons created from the superimposition of the favourable geological, hydrothermal alteration and magnetic relationships presented in Figures 19 to 23. The greater the number of overlapping features the greater the probability for the focussing of ascending magma and the development of a porphyry-system. The focus-scores are indicated by cyan (two overlaps), green (three overlaps), yellow (four overlaps) and red (five overlaps out of a possible six). The overlay shows the result of gridding the focus polygons using the minimum-curvature method in the surface grid tools available in Discover version 12.0. The focus-prospectivity grid is scored from moderate-prospectivity (cyan) to high-prospectivity (red).

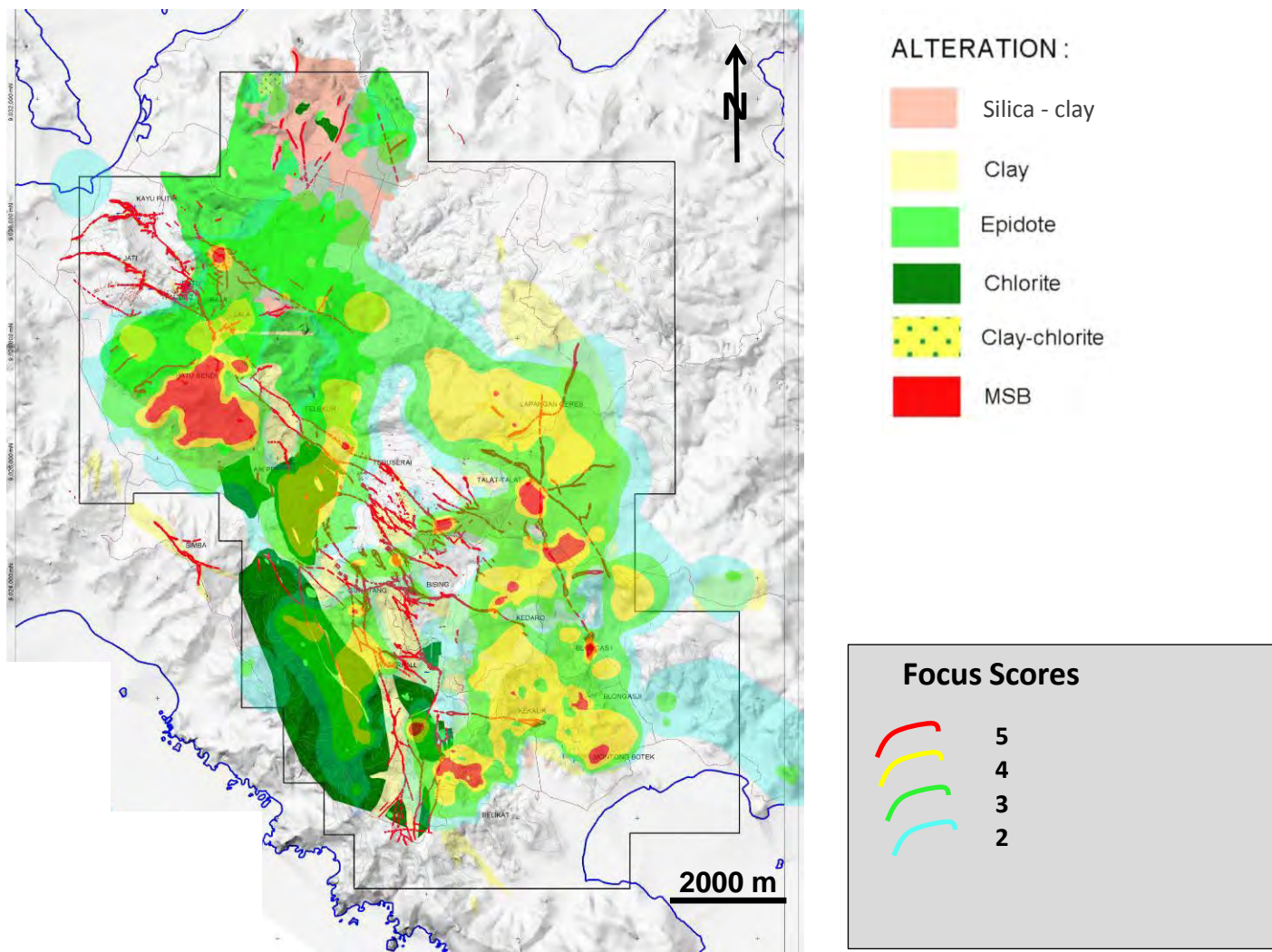


Figure 26: Pathway x focus scores shown on simplified geology for the SW Lombok IUP. The scores are derived by multiplying the pathway-scores by the focus-scores from the prospectivity maps presented in the preceding figures. If any area lacks a potential pathway or focus (i.e., either the pathway-score or focus-score equals zero), then the potential for a porphyry deposit is considered to be poor (the pathway x focus score equals zero). The scores range from moderate (cyan) to high (red and magenta). Zones prospective for porphyry-type mineralization occur in Motong Botek, Blongas, Mahoni, Belikat, Makam Kedaro, Bising, Lendak Bare, Telekur, Batu Sendi and Lala.

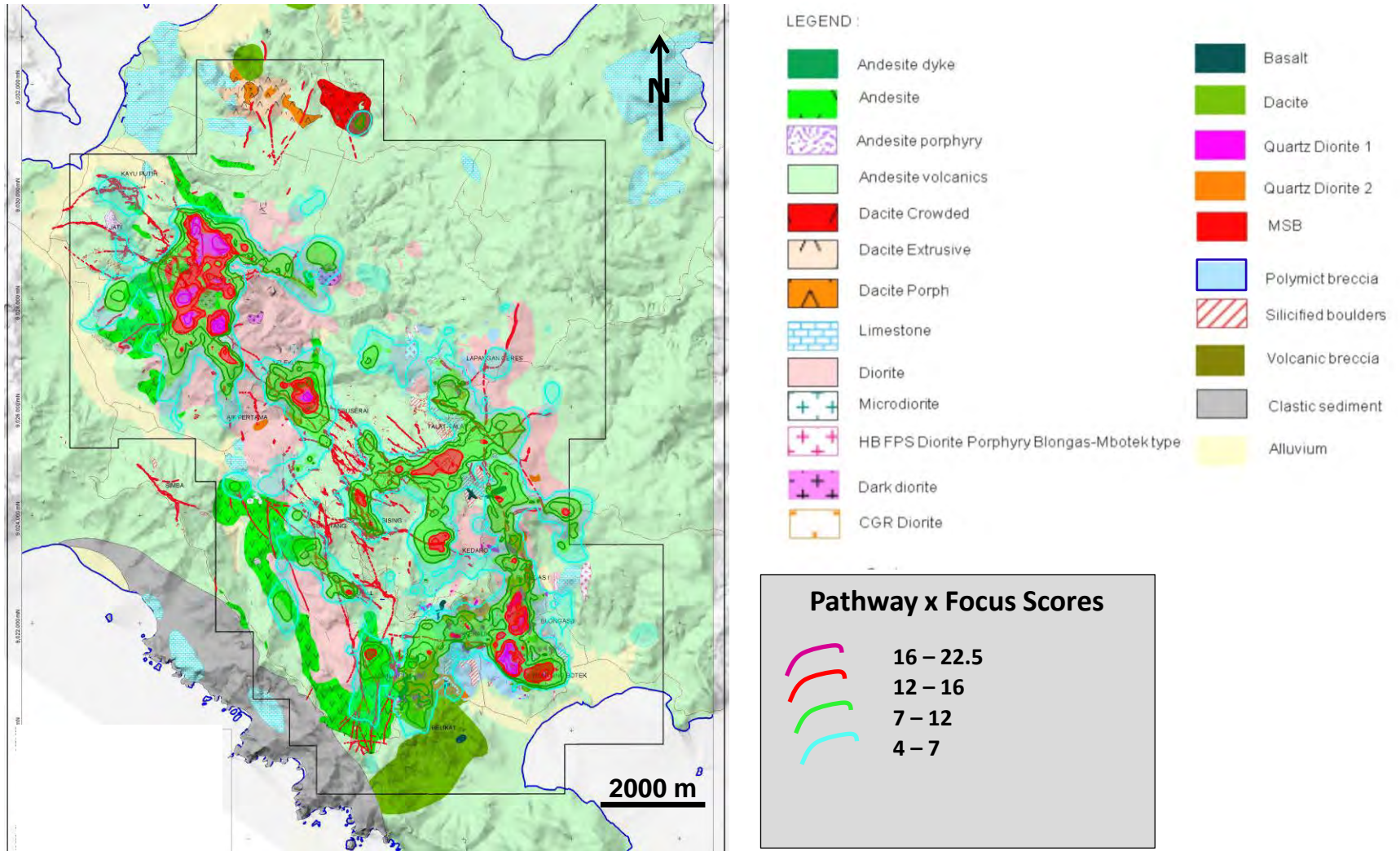


Figure 27: Pathway x focus scores shown on simplified hydrothermal alteration for the SW Lombok IUP. The scores are derived by multiplying the pathway-scores by the focus-scores from the prospectivity maps presented in the preceding figures. If any area lacks a potential pathway or focus (i.e., either the pathway-score or focus-score equals zero), then the potential for a porphyry deposit is considered to be poor (the pathway x focus score equals zero). The scores range from moderate (cyan) to high (red and magenta). Zones prospective for porphyry-type mineralization occur in Motong Botek, Blongas, Mahoni, Belikat, Makam Kedaro, Bising, Lendak Bare, Telekur, Batu Sendi and Lala.

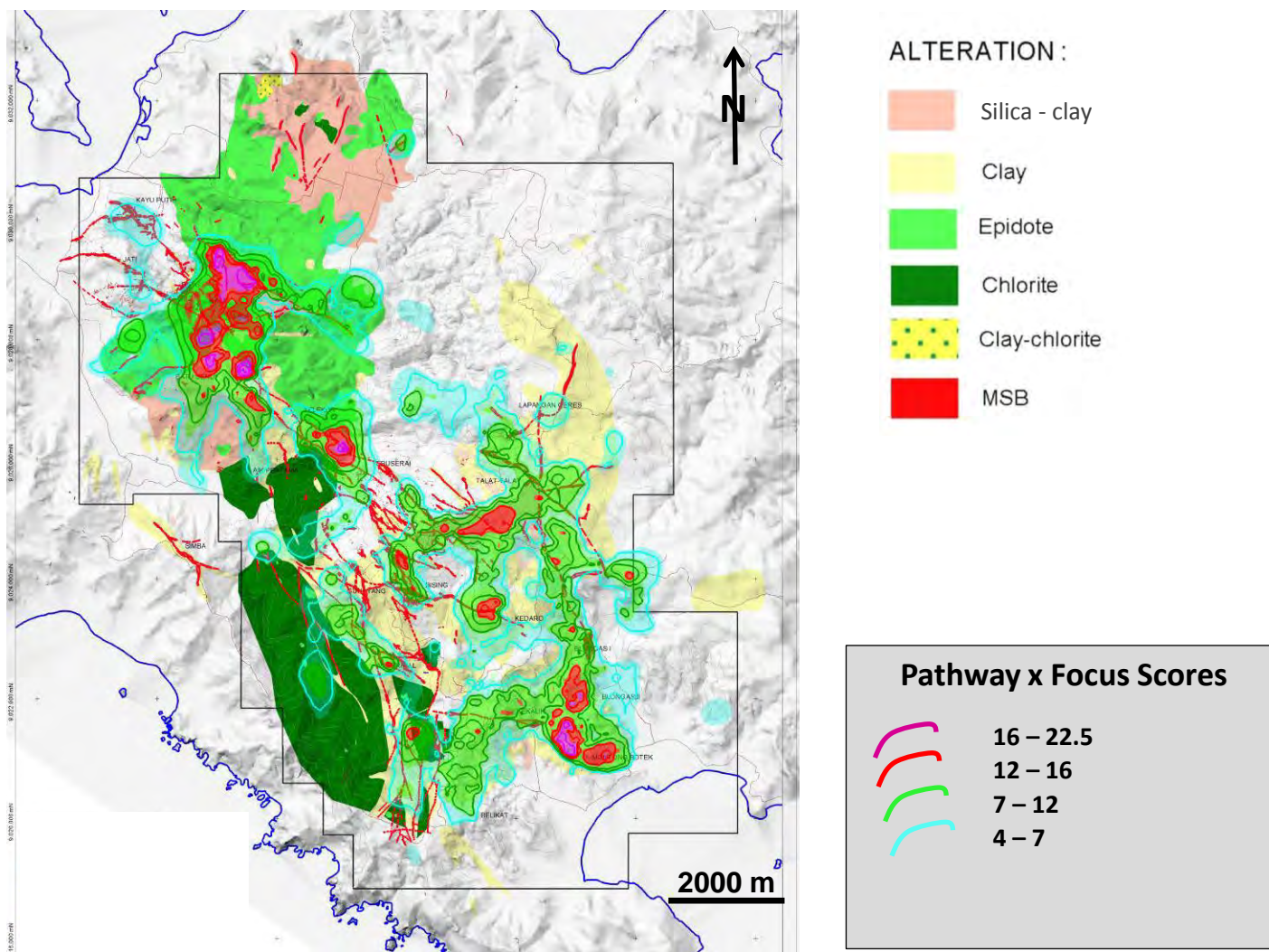


Figure 28: Proposed porphyry exploration targets and pathway x focus scores shown on simplified geology for the SW Lombok IUP. The targets are classified and ranked according to recommended future exploration program and prospectivity (refer to the table in Figure 30). The classifications are as follows: **A** = follow-up mapping required to delineate drill-targets; **B** = ridge and spur soil sampling necessary to advance targets; **C** = reconnaissance mapping to determine if target warrants additional work; and **D** = target previously tested by drilling. The targets are ranked by decreasing priority for each classification (i.e., 1 = high-priority and 4 = lower-priority).

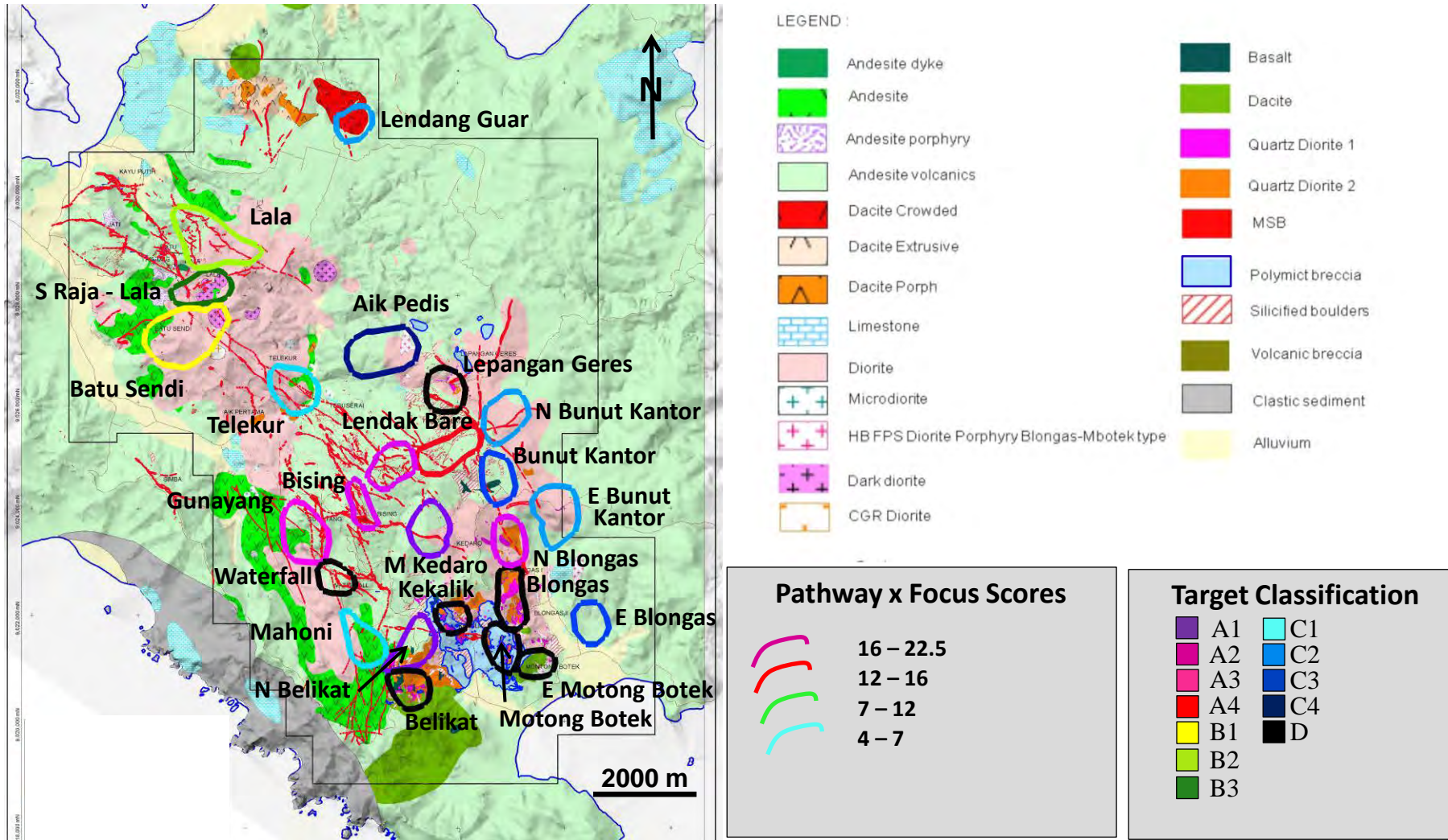


Figure 29: Proposed porphyry exploration targets and pathway x focus scores shown on simplified hydrothermal alteration for the SW Lombok IUP. The targets are classified and ranked according to recommended future exploration program and prospectivity (refer to the table in Figure 30). The classifications are as follows: **A** = follow-up mapping required to delineate drill-targets; **B** = ridge and spur soil sampling necessary to advance targets; **C** = reconnaissance mapping to determine if target warrants additional work; and **D** = target previously tested by drilling. The targets are ranked by decreasing priority for each classification (i.e., 1 = high-priority and 4 = lower-priority).

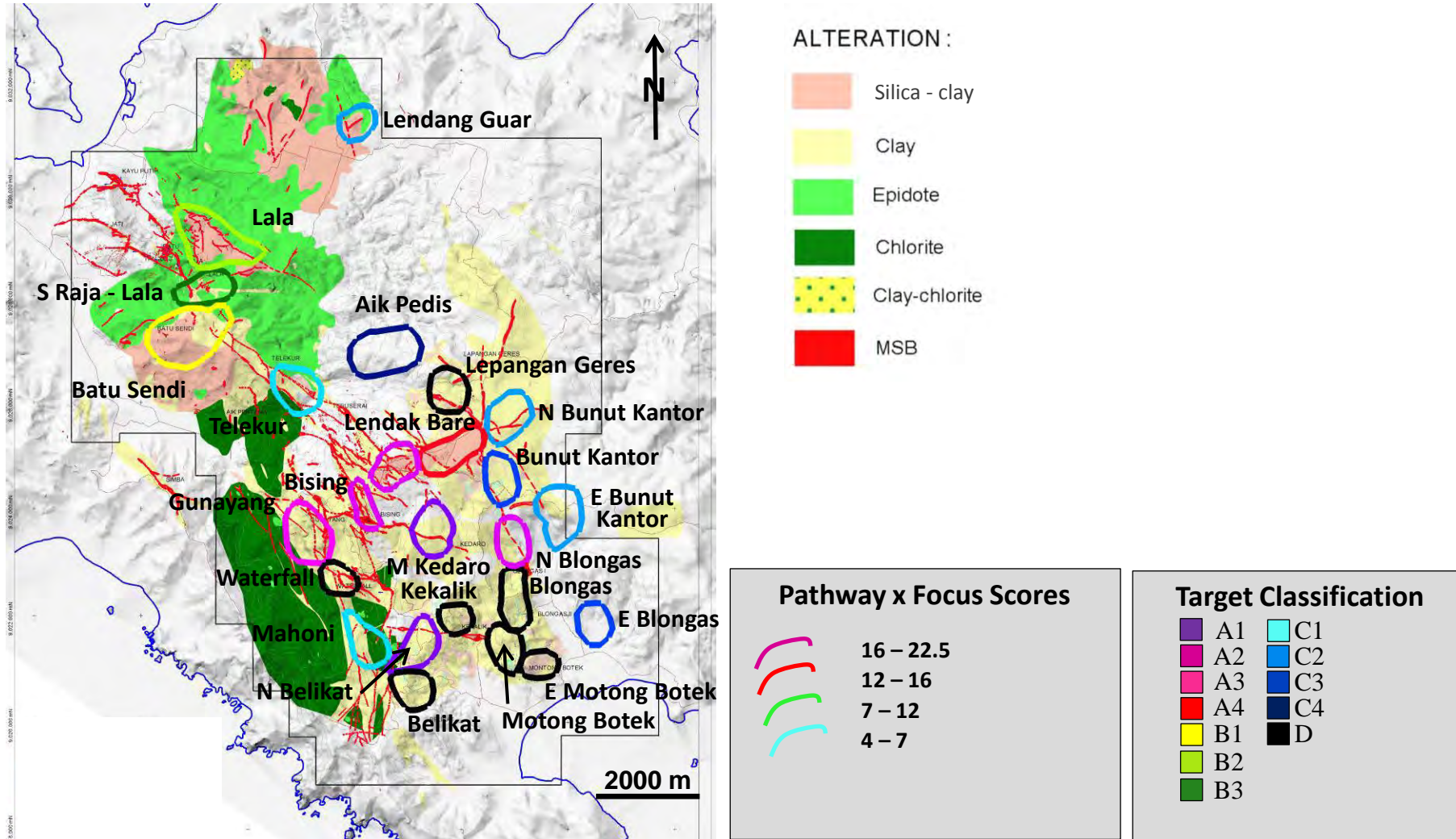


Figure 30: Proposed porphyry exploration targets for the SW Lombok IUP. The targets are classified according to recommended future exploration program: **A** = follow-up mapping required to delineate drill-targets; **B** = ridge and spur soil sampling necessary to advance targets; **C** = reconnaissance mapping to determine if target warrants additional work; and **D** = target previously tested by drilling. The targets are ranked by decreasing priority for each classification level (i.e., 1 = high-priority and 4 = lower-priority).

Target Name	Class / Rank	Exploration Recommendations
Makam Kedaro	A1	mapping and drilling
North Belikat	A1	mapping and drilling
West Lendak Bare	A2	mapping, clay sampling and drilling
Bising	A2	mapping and drilling
North Blongas	A2	mapping
Gunayang	A3	mapping
East Lendak Bare	A4	mapping and clay sampling
Batu Sendi	B1	mapping and r/s soil sampling
Lala	B2	mapping and r/s soil sampling
South Raja – Lala	B3	mapping and r/s soil sampling
Telekur	C1	mapping and r/s soil sampling?
Mahoni	C1	recon mapping
Lendang Guar	C2	recon mapping
East Bunut Kantor	C2	recon mapping
North Bunut Kantor	C2	recon mapping
Bunut Kantor	C3	recon mapping
East Blongas	C3	recon mapping
Aik Pedis	C4	recon mapping
Motong Botek	D	previously tested by multiple DDH
East Motong Botek	D	previously tested by one DDH
Blongas	D	previously tested by multiple DDH
Kekalik	D	previously tested by two DDH
Belikat	D	previously tested by four DDH
Lepangan Geres	D	previously tested by three DDH
Waterfall	D	previously tested by multiple DDH

Figure 31: Proposed porphyry exploration targets shown on deep-level magnetics / inferred diorite pluton image for the SW Lombok IUP. The targets are classified and ranked according to recommended future exploration program and prospectivity (refer to the table in Figure 30). The classifications and rankings are explained in the previous figures. The most prospective porphyry-systems drilled to date (Motong Botek and Blongas) occur near the margin of the deep-level magnetic high / diorite pluton in the Selodong – Mencanggih area. Several targets have yet to be drill-tested that also sit near this same margin. These include the A-class targets of North Belikat, Bising, West and East Lendak Bare, and Gunayang; and the C-class targets of North Bunut Kantor and East Blongas. The B-class targets in the Batu Sendi, South Raja and Lala areas lie within mapped diorite near the western margin of the deep-level magnetic body. The Telekur target lies along the south-eastern margin of this northern diorite body. Completed drill-holes are indicated by the grey line-traces.

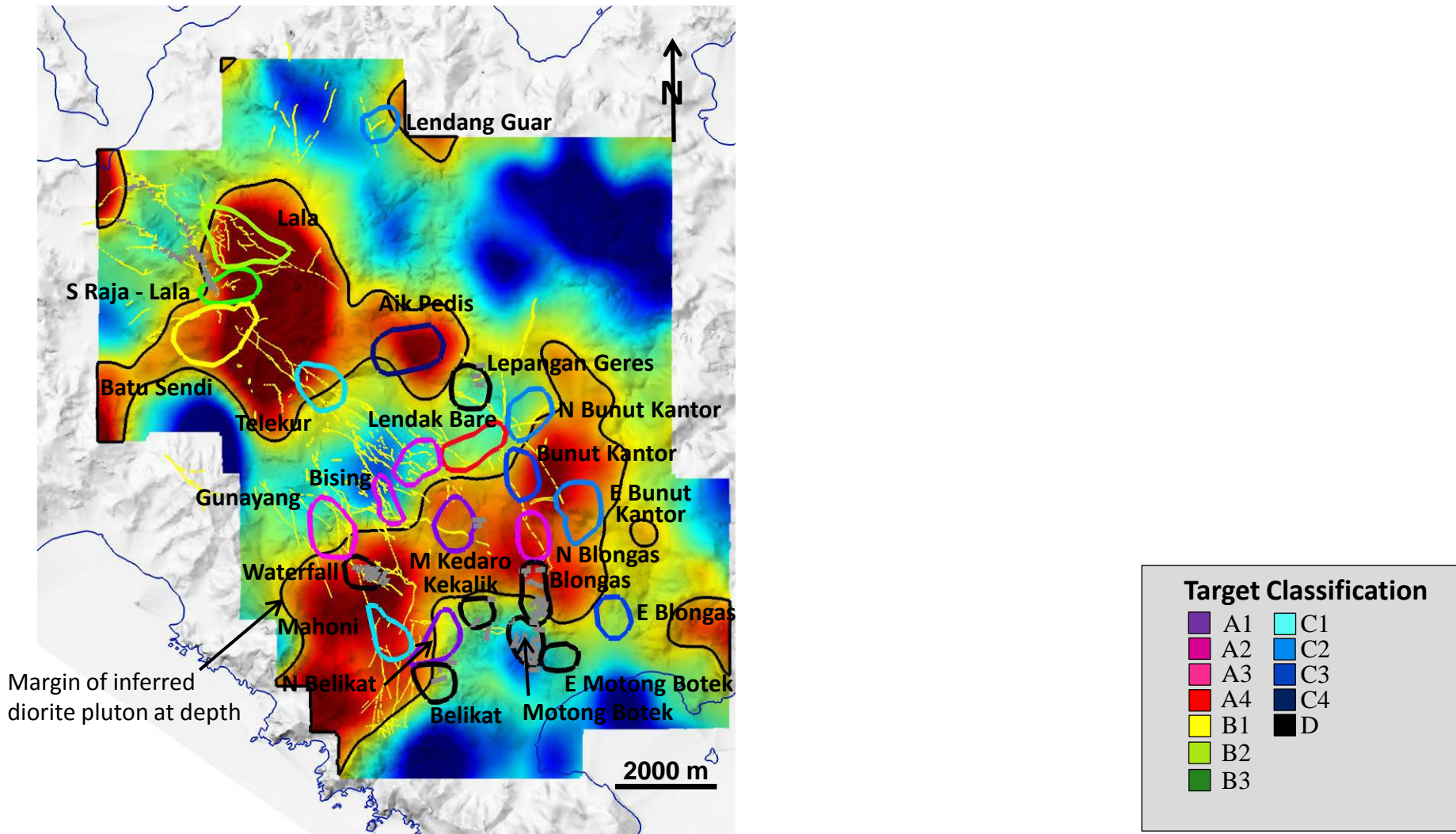


Figure 32: Proposed porphyry exploration targets and three-dimensional magnetic inversion models for the SW Lombok IUP. Eleven models were produced by Fathom Geophysics (2011). The transparent yellow shells indicate moderate magnetic-susceptibilities, typically 0.02 to 0.04 SI units; the solid orange shells indicate higher magnetic-susceptibilities, generally characterized by 0.04 to 0.08 SI units. The Bising model is expressed by a lower magnetic response: 0.015 (yellow) and 0.02 SI units (orange). Completed drill-holes are indicated by the grey line-traces. The following figures illustrate the relationships between the magnetic inversions and proposed targets in greater detail.

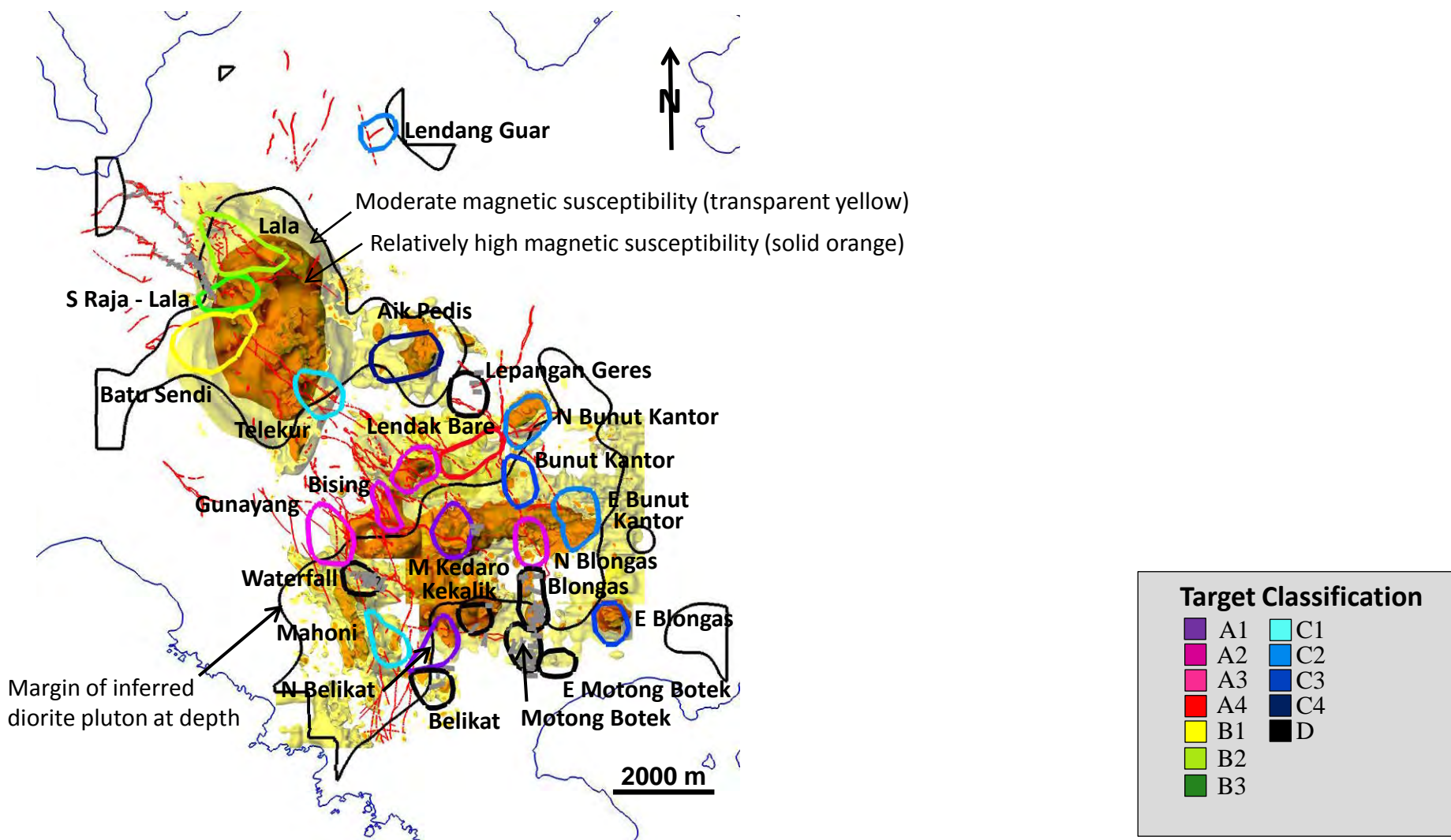


Figure 33: Oblique-view (looking -60° towards $N50^\circ W$) of proposed porphyry exploration targets and three-dimensional magnetic inversion models for the northern part of the SW Lombok IUP. The transparent yellow shells indicate moderate magnetic-susceptibilities (0.04 SI units); the solid orange shells indicate higher magnetic-susceptibilities (0.08 SI units). The surface outlines of equigranular diorite (magenta), dark (unaltered) diorite (black), microdiorite (green) and hornblende diorite (pink – Aik Pedis) typically coincide with magnetic highs. Prospective magnetic highs that are not directly explained by magnetic diorites occur in the northern part of the Lala target, the south-eastern part of Batu Sendi, central Aik Pedis and at Telekur. Completed drill-holes are indicated by the grey line-traces. The topographic contour interval is 25 m.

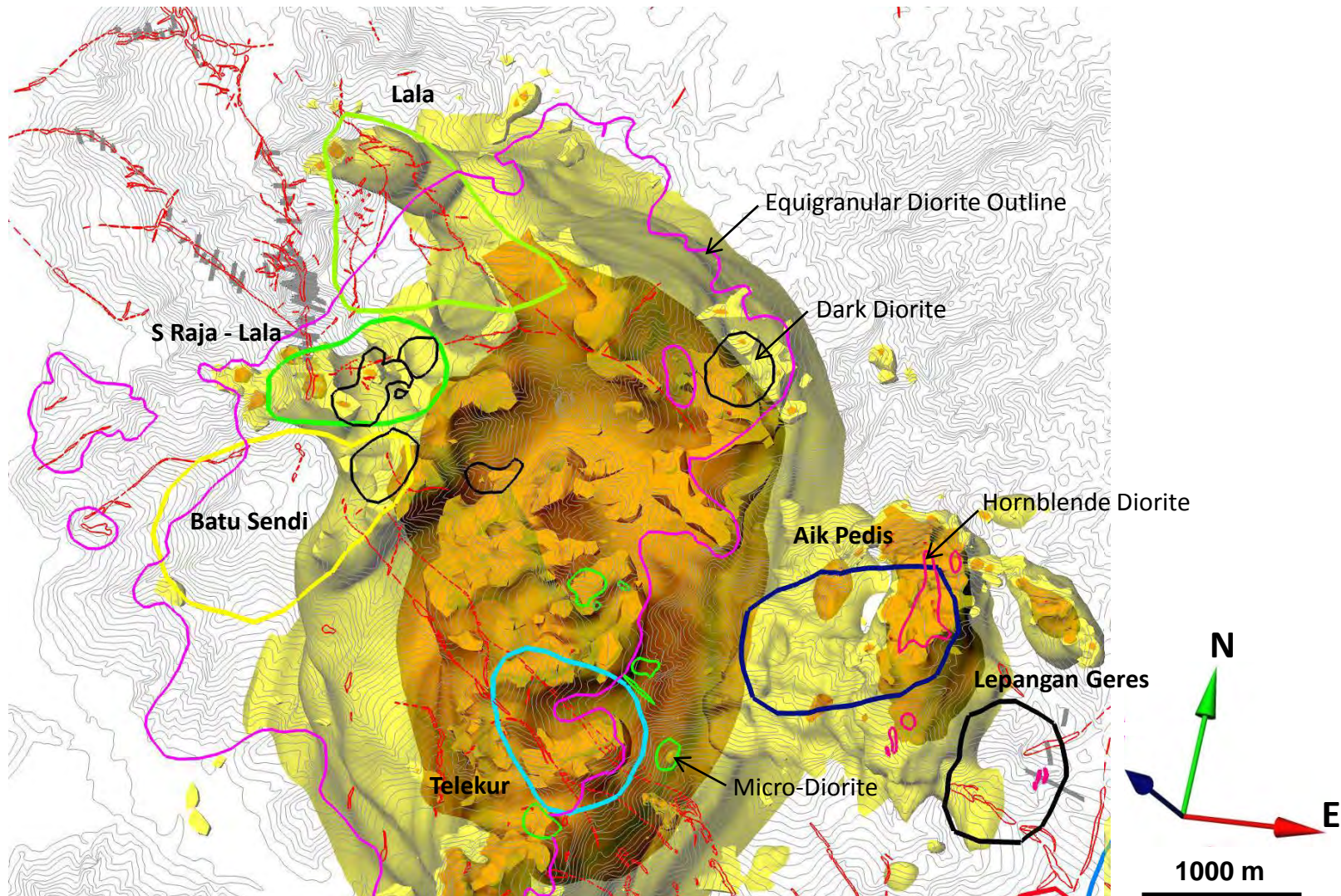


Figure 34: oblique-view (looking -60° towards $N50^\circ W$) of proposed porphyry exploration targets and three-dimensional magnetic inversion models for the northern part of the SW Lombok IUP. The transparent yellow shells indicate moderate magnetic-susceptibilities (0.04 SI units); the solid orange shells indicate higher magnetic-susceptibilities (0.08 SI units). The surface outlines of silica-clay alteration zones are indicated by the transparent magenta polygons. Spectral (SWIR) analyses show that the northern part of Batu Sendi contains variable amounts of dickite, alunite and pyrophyllite, which indicate a high-temperature advanced argillic (low pH) alteration assemblage (pyrophyllite is stable above $300^\circ C$). The Lala silica-clay zone contains kaolinite, dickite and alunite, which indicates advanced argillic alteration $< 300^\circ C$. The southern part of Batu Sendi is characterized by illite and minor paragonite, which indicates near-neutral pH conditions. Completed drill-holes are indicated by the grey line-traces. The topographic contour interval is 25 m.

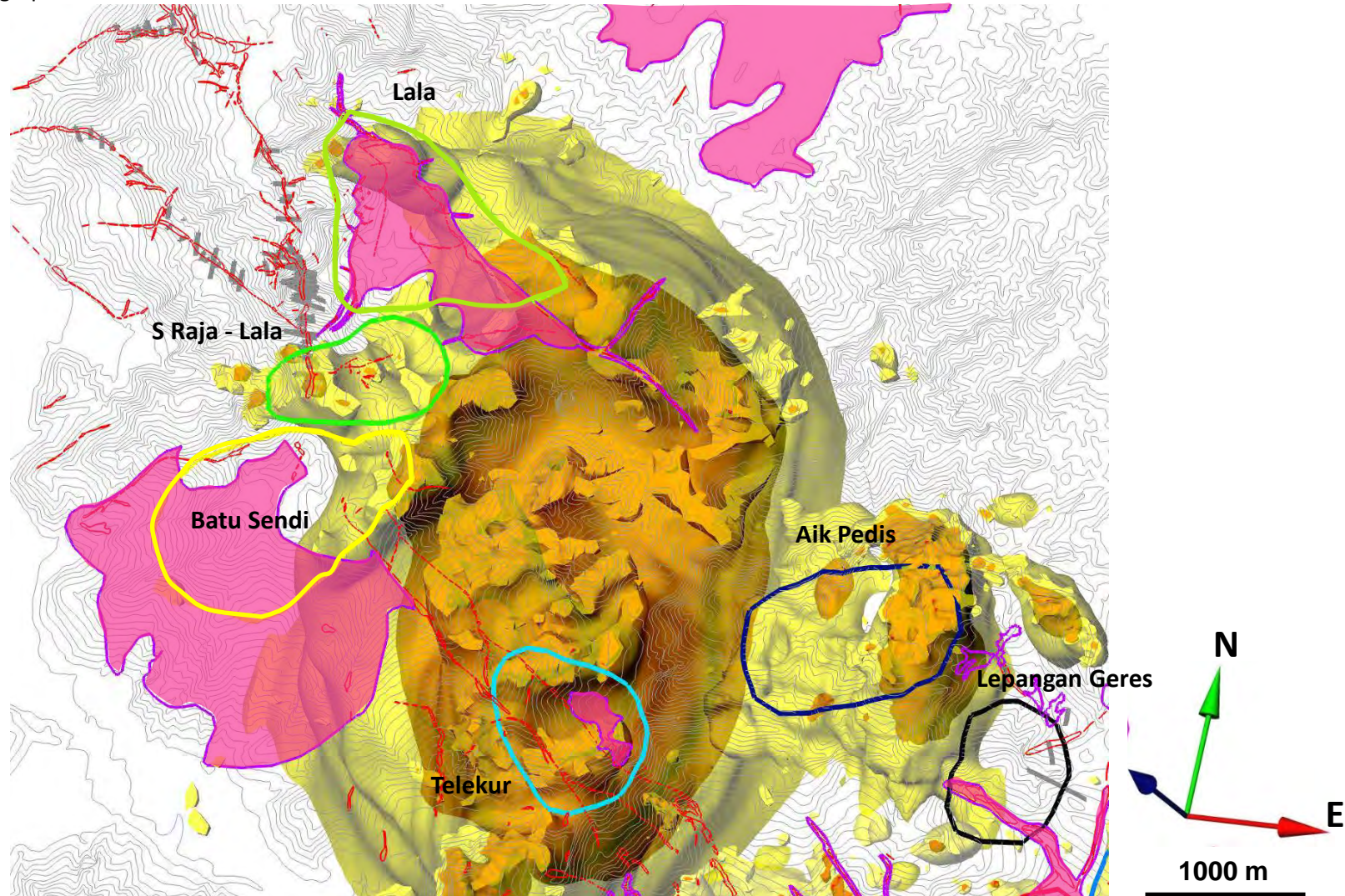


Figure 35: Oblique-view (looking -35° towards $N55^\circ E$) of proposed porphyry exploration targets and three-dimensional magnetic inversion models for the central part of the SW Lombok IUP. The transparent yellow shells indicate low- to moderate-magnetic-susceptibilities (typically 0.015 to 0.02 SI units); the solid orange shells indicate higher magnetic-susceptibilities (0.02 to 0.04 SI units). The surface outlines of silica-clay alteration zones are indicated by the transparent magenta polygons. Spectral (SWIR) analyses indicate that the alteration zones at Bising and West Lendak Bare contain pyrophyllite, diaspore, dickite and alunite (high-temperature, advanced argillic alteration). The silica-clay zone at West Lendak Bare has yet to be sampled. Discrete magnetic-highs occur in the southern part of Bising West Lendak Bare, Kedaro and North Bunut Kantor targets. Completed drill-holes are indicated by the grey line-traces. The topographic contour interval is 25 m.

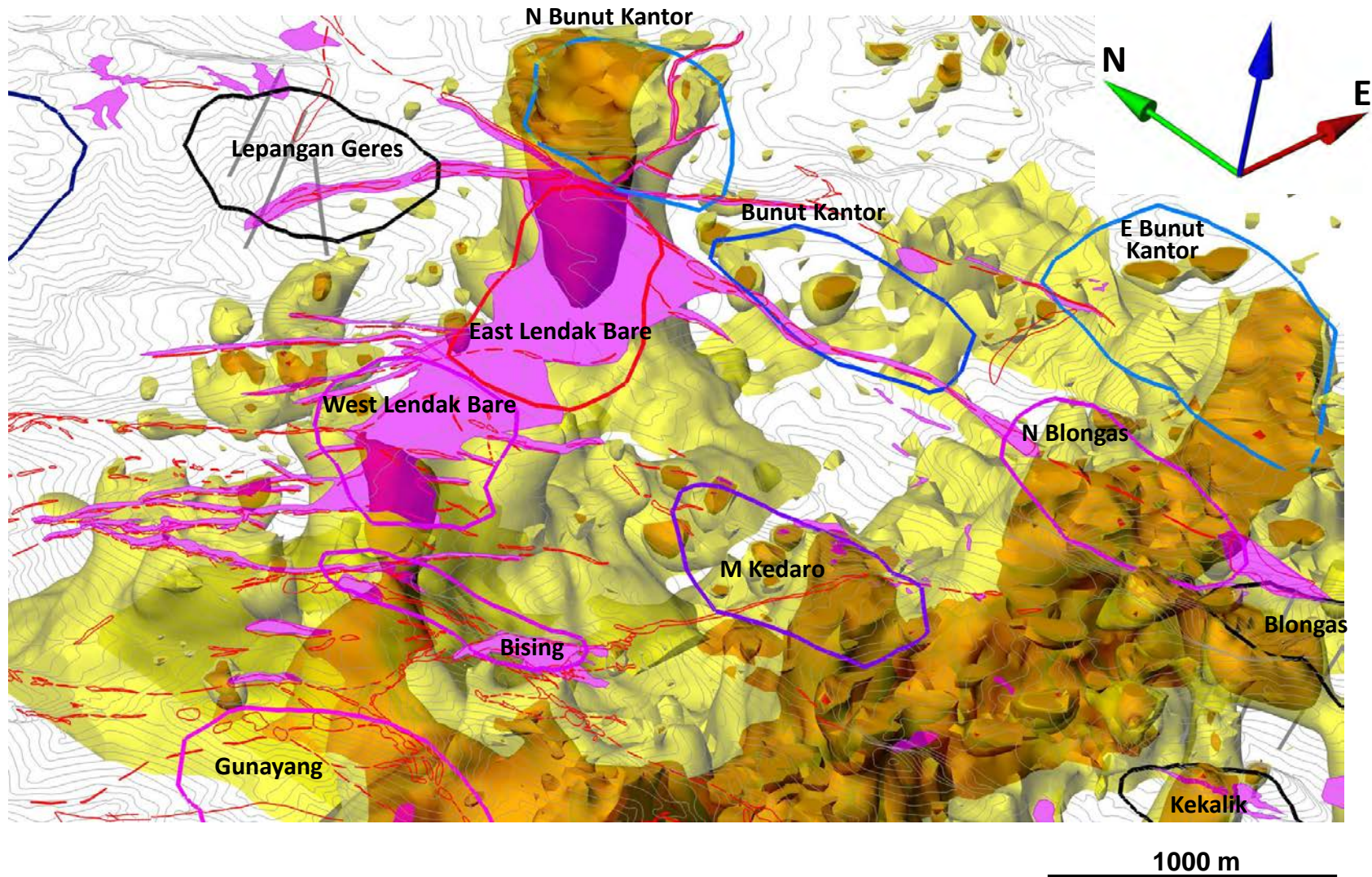


Figure 36: Oblique-view (looking -35° towards $N55^\circ E$) of proposed porphyry exploration targets and three-dimensional magnetic inversion models for the central part of the SW Lombok IUP. The transparent yellow shells indicate low- to moderate-magnetic-susceptibilities (typically 0.015 to 0.02 SI units); the solid orange shells indicate higher magnetic-susceptibilities (0.02 to 0.04 SI units). The surface outlines of molybdenum-in-soil of 6 – 20 ppm (light green) and 20 – 50 ppm (dark green) show discrete anomalies over Bising, Gunayang, Makam Kedaro and North Blongas. Completed drill-holes are indicated by the grey line-traces. The topographic contour interval is 25 m.

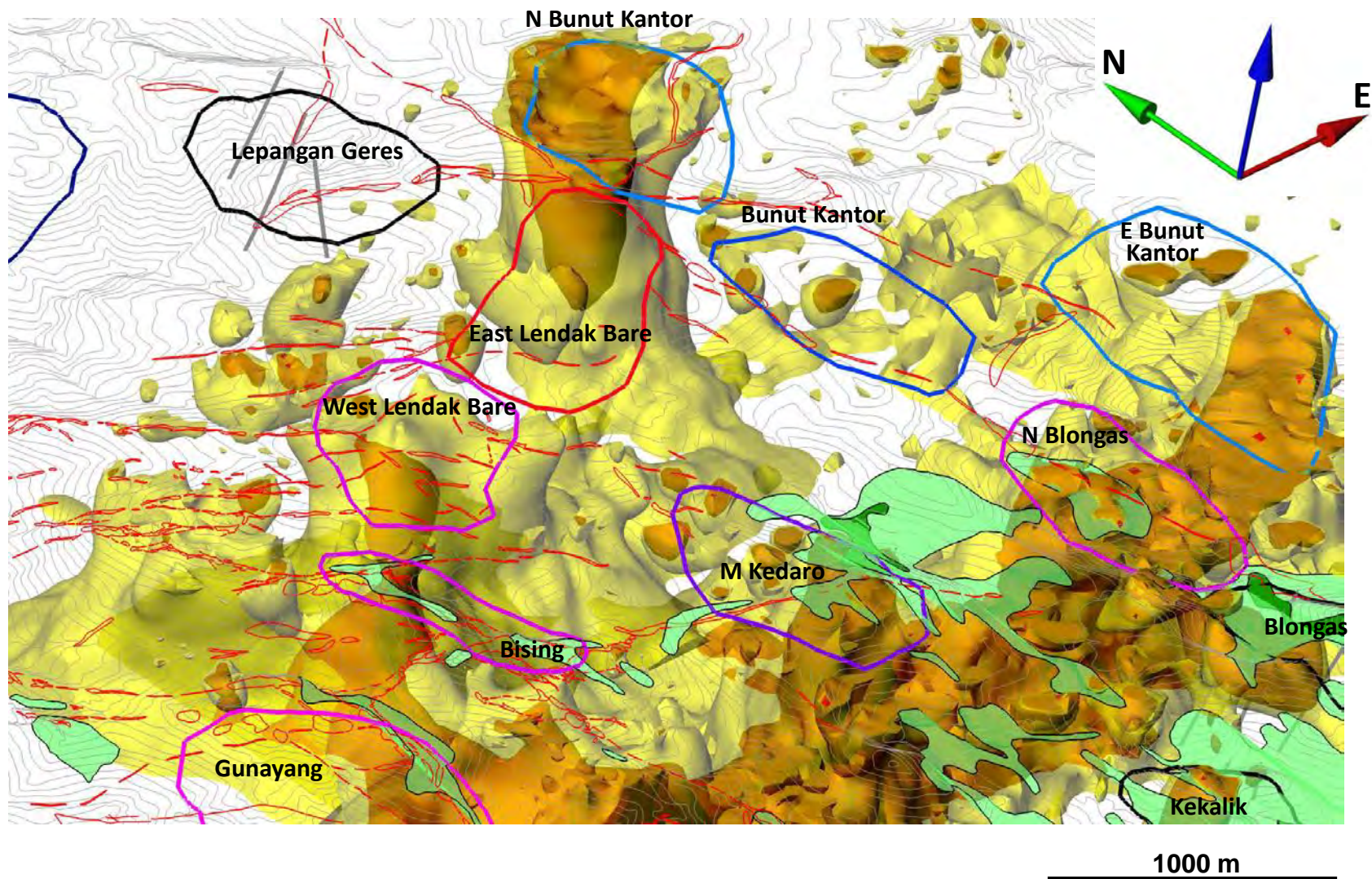


Figure 37: Oblique-view (looking -20° towards $N50^\circ W$) of the Bising and West Lendak Bare porphyry targets, showing magnetic inversion models, silica-clay alteration zones (semi-transparent pink polygons) and quartz-ledges / MSBs. The transparent yellow shells indicate low- to moderate-magnetic-susceptibilities (0.015 to 0.02 SI units); the solid orange shells indicate higher magnetic-susceptibilities (0.02 to 0.04 SI units). Both target areas contain discrete magnetic highs that are consistent with cupolas above a porphyry system. The apex of the Bising magnetic-high is at 220 m RL or 180 m below surface; the apex of the West Lendak Bare magnetic-high reaches 320 m RL or 120 m below surface. The topographic contour interval is 25 m.

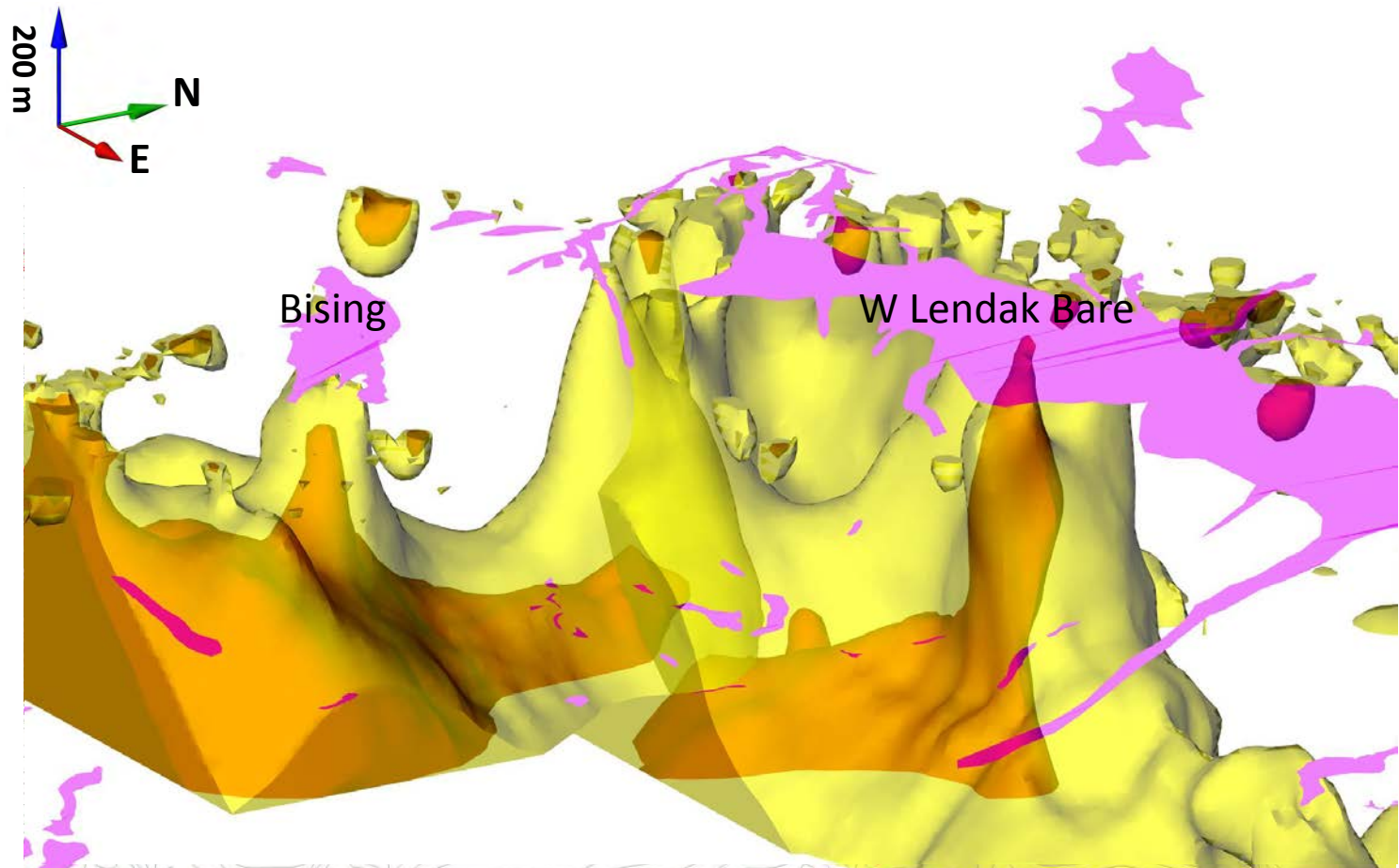


Figure 38: Oblique-view (looking -48° towards $N20^\circ E$) of proposed porphyry exploration targets and three-dimensional magnetic inversion models for the Selodong area in the southern part of the SW Lombok IUP. The transparent yellow shells indicate low- to moderate-magnetic-susceptibilities (typically 0.02 to 0.04 SI units); the solid orange shells indicate higher magnetic-susceptibilities (0.03 to 0.08 SI units). The surface outlines of silica-clay alteration zones are indicated by the transparent magenta polygons. Discrete magnetic-highs occur in the Bising, Makam Kedaro, Belikat, North Belikat, Kekalik, Mahoni, Motong Botek, Blongas and East Blongas. Completed drill-holes are indicated by the grey line-traces. The topographic contour interval is 25 m.

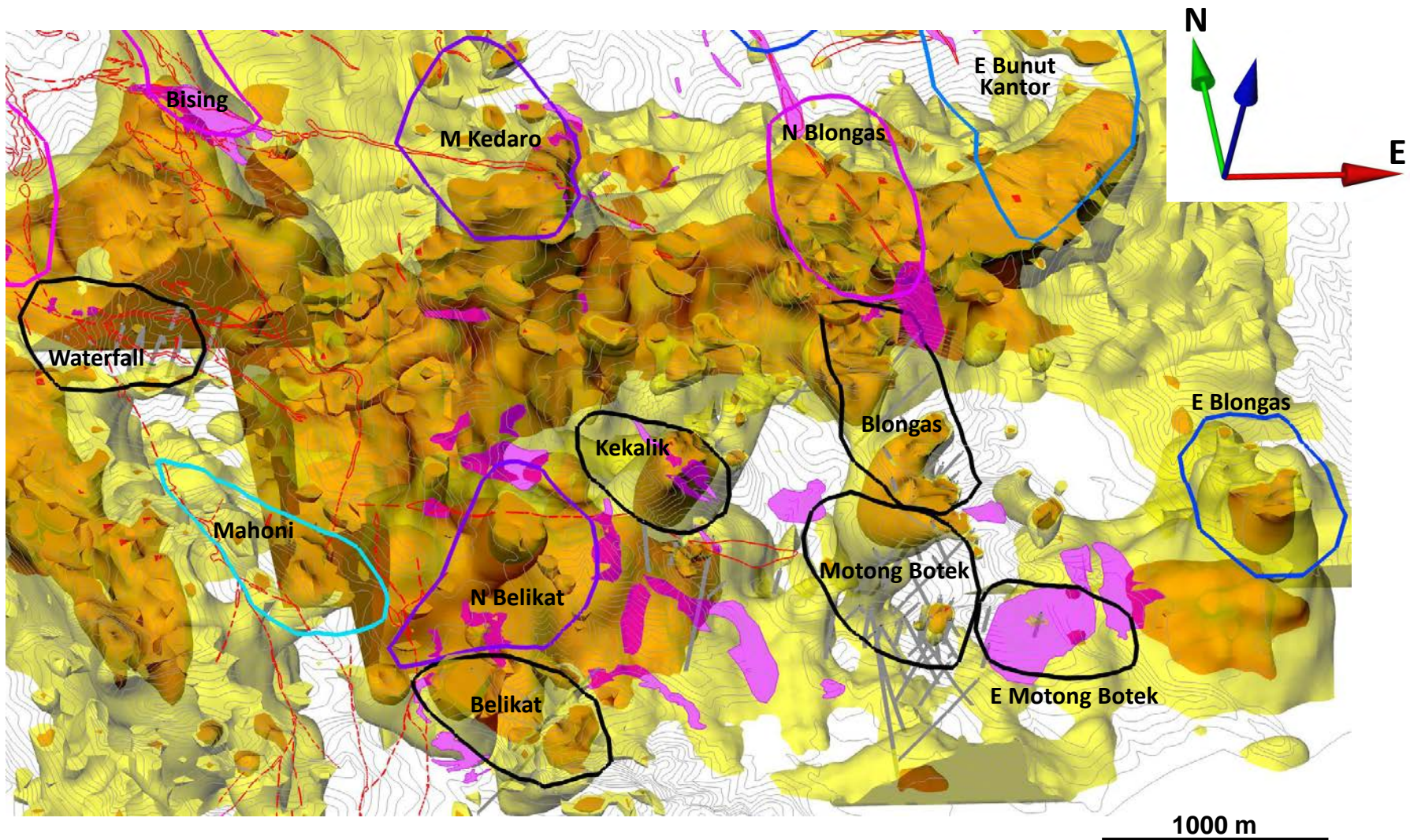
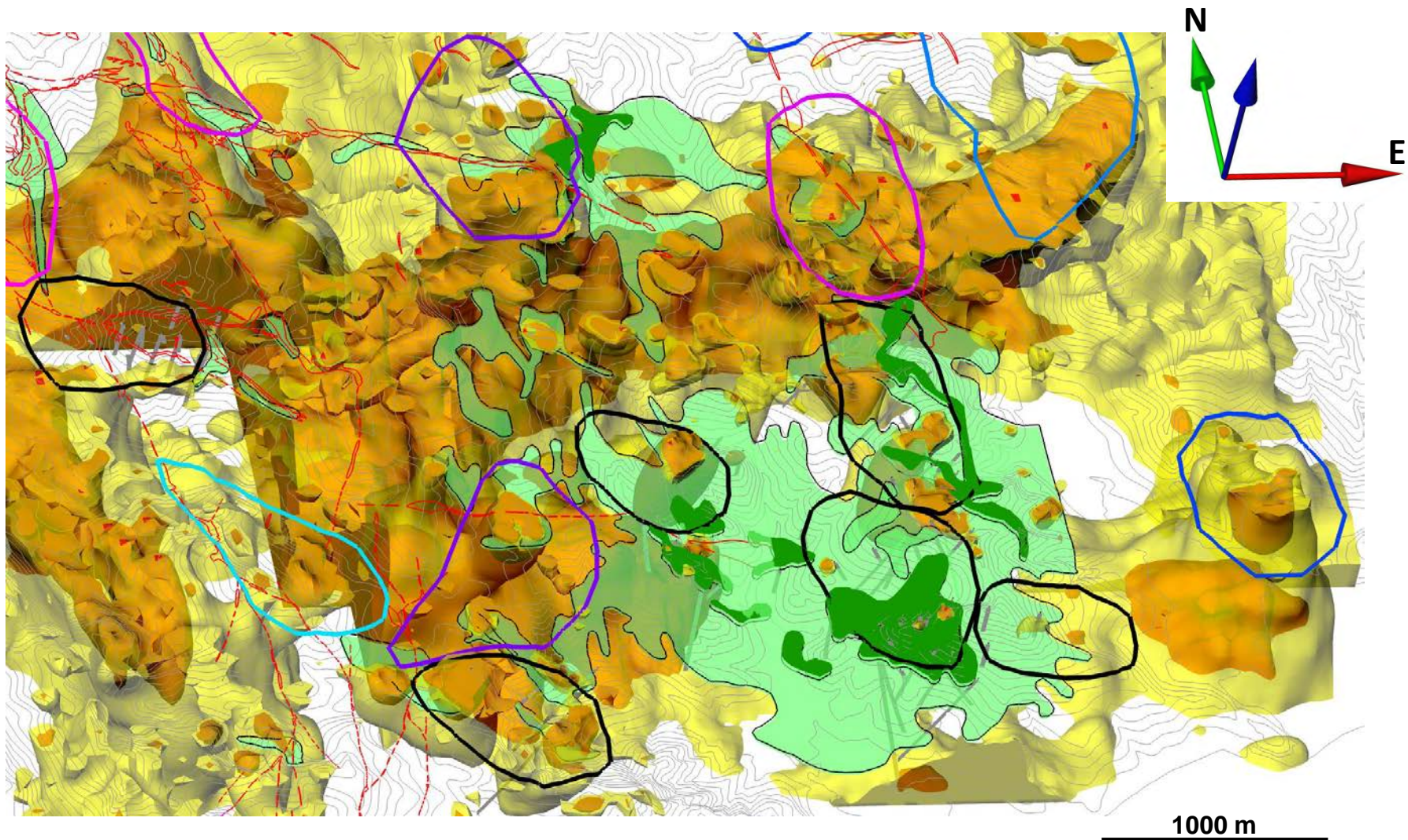


Figure 39: Oblique-view (looking -48° towards $N20^\circ E$) of proposed porphyry exploration targets and three-dimensional magnetic inversion models for the Selodong area in the southern part of the SW Lombok IUP. The transparent yellow shells indicate low- to moderate-magnetic-susceptibilities (typically 0.02 to 0.04 SI units); the solid orange shells indicate higher magnetic-susceptibilities (0.03 to 0.08 SI units). The surface outlines of molybdenum-in-soil of 6 – 20 ppm (light green) and 20 – 50 ppm (dark green) show discrete anomalies over Bising, North Blongas, Blongas, Motong Botek, Kekalik, and Belikat. Completed drill-holes are indicated by the grey line-traces. The topographic contour interval is 25 m.



Porphyry Exploration Potential, SW Lombok

Conclusions and Recommendations

- Spatial coincidence between major geological-, topographic- and geophysical-lineaments
 - Geology controls topographic and magnetic expressions
 - Combined lineament density used as an indication of favorable pathways for porphyry emplacement
- Intrusion distribution, magnetic / radiometric expression and silica-clay alteration indicate zones of focused magmatic-hydrothermal fluid-flow
 - Diorite pluton margins, quartz diorites and dacite porphyries, high-level magnetic highs above or adjacent to deep-magnetic bodies, silica-clay alteration zones and zones of low K/Th radiometric response indicate focus zones
- Eighteen untested porphyry targets created on basis of prospectivity analysis
 - Pathway x focus scores, three-dimensional magnetic inversions and molybdenum-in-soil results used to generate exploration targets
 - Targets classified by recommended future exploration program and ranked by prospectivity within each target class
 - The most prospective targets include Makam Kedaro, North Belikat, Bising and West Lendak Bare (A-class); Batu Sendi and Lala (B-class); and Mahoni and Telekur (C-class).
- Future exploration to include mapping, rock- and soil-sampling, and SWIR-clay analyses
 - Detailed mapping (~ 1:2000-scale) of A- and B-class targets to focus on abundance / orientation of porphyry-style quartz veins and fractures, distribution of quartz-bearing porphyritic intrusions and dike swarms
 - Ridge and spur soil sampling in B-Class targets to determine if metal zoning is present (e.g., central Cu-Au, proximal Mo and distal Zn)
 - Consider pyrophyllite-alunite-dickite-bearing silica-clay zones as potential lithocaps to porphyry systems
 - Reconnaissance mapping (~ 1:5000-scale) of C-class targets to determine potential and future exploration program